Spectroscopy of a Many Josephson Junction System using Inelastic Cooper Pair Tunneling

M. Sc. Thesis

Juha Leppäkangas
University of Oulu
Department of Physical Sciences
Theoretical Physics

Oulu 2003

Contents

Chapter 1

Introduction

After quantum mechanics was formulated in the beginning of the 20th century, it was discussed whether or not quantum effects could be present at the macroscopic scale too. Could a certain macroscopic system have a quantized energy spectrum and quantum evolution of a superposition of states, even if it describes the collective state of a macroscopic number of particles? Or does quantum mechanics always reduce to classical mechanics at the macroscopic scale? The question was fascinating but it took many decades before it was a matter of experimental physics. The idea was boosted again in the beginning of the 1980s, when it was discussed that macroscopic quantum phenomena could finally be realized in experiments also [1, 2]. The realization was based on the Josephson effect, an important phenomenon originally found in the 1960s.

The Josephson effect can occur between two superconductors, if they are separated by a thin insulator. Such a connection is called the Josephson junction. In the superconducting state, a metal has no resistance and a current can flow when no voltage is applied. This is a consequense that electrons tend to form bound pairs in certain metals at very low temperatures, $T \sim 1$ K. One bound pair, called a Cooper pair, has the charge $-2e$ and zero spin. So one could view that a Cooper pair is a boson and therefore it tends to be in exactly the same state with other Cooper pairs, resulting an unanimous and nondissipative current flow. The system is very coherent, even though it is formed from a macroscopic number of electrons, all the Cooper pairs are in the same "phase" state. In the Josephson effect, if $V \neq 0$ between the leads, there is a coherent ac-supercurrent through the insulating barrier, resulting no net current over time. If we maintain $V = 0$, a dc-current will flow through the system, depending sinusoidally on the phase difference between the superconductors. This weird current-voltage behaviour is a result of a quantum mechanical coupling between the Cooper pairs at different sides of the insulating barrier.

The Josephson phenomenon in itself is described by a semiclassical the-

ory, but it was later predicted that new effects should arise at low temperatures for mesoscopic junctions. In that case, the behaviour of the junction should be described completely quantum mechanically rather than by using the semiclassical theory. In this limit the collective state of a macroscopic number of electrons should show quantum effects. Manufacturing such mesoscopic junctions and establishing suitable conditions for observing the macroscopic quantum phenomenon (MQP) was not possible until at the beginning of the 1980s. Afterwards, there has been plenty of experimental evidences for the fact that MQP is present in small Josephson junction systems. There has been observations of energy level quantaziation (ELQ), macroscopic quantum tunneling (MQT), macroscopic quantum coherence (MQC) of two states and of many states also. Most of the research has been done for observing MQT of the phase difference φ between two superconductors. SQUID devices (which consist of two Josephson junctions parallel in a magnetic field) coupled to an inductor have also verified the existence of MQT, ELQ and MQC.

The Josephson effect is based on a coherent Cooper pair transfer over the insulating barrier. In the semiclassical model of the Josephson effect, the discreteness of its basic event, the transfer of a single Cooper pair over the insulating barrier, can be forgotten. But when dealing with small junctions and for example a weak Josephson coupling energy, it can have a major impact on the current-voltage charasteristics of the system. Observation of a Coulomb blockade is a manifestation that a change of a single charge in the tunneling region can be forbidden and it therefore blocks the current from a macroscopic number of Cooper pairs, resulting in a total absence of the tunneling. Another important phenomenon when dealing with the small Josephson coupling energy is the inelastic Cooper pair tunneling. It manifests the energy exchange between the Josephson junction and its electromagnetic environment when a Cooper pair tunnels over the insulating barrier. As a result, the tunneling leaves traces from the environment's energy structure to the current-voltage characteristics of the system. Thus inelastic Cooper pair tunneling can be used to probe the energy levels of the environment.

The MQP is not only interesting to study, but it could also have effective applications in future. For example, it is thought and partly shown that small Josephson junctions could be used as a basis of quantum computers [3]. Increase of the calculation power in ordinary computers is achieved by decreasing the size of a transistor. But at the end there's a limit when going to smaller and smaller sizes, the wave property of electrons. At some stage, the transistor cannot work anymore without errors. If one wants to increase the calculation power even further, the quantum computing is the answer. The basic idea in the quantum computer is to use the quantum evolution of a superposition of states as a calculation method. Josephson junction based systems could be ideal for acting as quantum bits in the quantum computers,

or in other this kind of applications, because they are easily coupled to the electrical circuit. There has been a lot of similar research for normal state junctions (not superconducting) also in which electrons, instead of Cooper pairs, tunnel incoherently over the insulating barrier. However, normal state junctions are not the subject of this thesis.

My master's thesis is motivated by the experiments and research done by R. Lindell *et al.* for mesoscopic Josephson junctions, in Low Temperature Laboratory of Helsinki University of Technology. In the experiments, an inelastic tunneling of Cooper pairs is probably observed and with the help of that one is able to study the energy level structure of the SQUIDs. This is the first time when ELQ of the Josephson junctions is studied using this method. Surprisingly, also the semiclassical treatment of the same situation gives raise to very analogous current-voltage characteristics, even the two cases manifest completely different phenomena. Therefore a comparative analysis needs to be made. The purpose of this thesis is to study the behaviour of voltage biased many Josephson junction systems both semiclassically and quantum mechanically. $I-V$ characteristics of the systems are calculated numerically for both of the cases and then compared with the experimental data. Also the effect of an energy band structure of the SQUID, which was interpreted to be seen in these experiments, to inelastic tunneling of Cooper pairs is analyzed.

The stucture of the thesis is as follows. Chapter 2 gives the introduction to the semiclassical Josephson effect. Chapter 3 considers the peaks in the $I-V$ characteristics arising under rf-irradiation or in asymmetric many Josephson junction situations, numerical results for the $I-V$ curves are analyzed for different parameters. In chapter 4 we switch to the quantum mechanical treatment of the Josephson effect which is relevant when dealing with small Josephson junctions. Chapter 5 concentrates to the theory of inelastic Cooper pair tunneling. In chapter 6 we describe many Josephson junction systems in the same fashion as done in the $P(E)$-theory and discuss the effect of the gate voltage and the band structure. Chapter 7 contains the comparison between the models and experiments. A discussion is given in chapter 8.

Chapter 2

Classical Josephson Effect

We start our discussion from the semiclassical Josephson effect, which we will now on call simply the classical Josephson effect. It can be understood qualitatively with the help of the macroscopic view of superconductivity, the Ginzburg-Landay theory. Therefore we start by discussing the basics of superconductivity and then show how the Josephson effect arises. After that we show the equivalence between an isolated Josephson junction and an LC-oscillator. The SQUID is probably the most important application of superconductivity and will be discussed next. Finally we take into account the effect of quasiparticles and describe the junction's dynamics using the RCSJ-model. The treatment of this chapter is partly based on the discussions made by Feynman and Tinkham [4, 5], which are nice literature for beginners to read.

2.1 Macroscopic View of Superconductivity

The Josephson effect was originally predicted by Brian D. Josephson in 1962 [6]. At first, this brave derivation gave rise to a lot of sceptism, but a year later when Anderson and Rowell reported the very first observation of the Josephson effect [7], the theory was accepted. It turned out to be so crucial effect of superconductivity that Josephson shared the 1975 Nobel Prize for his work.

The Josephson effect can be understood using the ultimate coherence of superconductors. According to the microscopic model of superconductivity, the BCS-theory [8], in a superconducting state electrons form bound pairs due to a weak attractive force resulting from complicated electron-phonon interactions. These bound pairs are called Cooper pairs, they carry a charge $-2e$ and have zero spin. One can now interpretate that because Cooper pairs have no spin they act as they were bosons. As a result, the system is analogous to the Bose-Einstein condensation at low temperatures: all the Cooper pairs are in the same quantum mechanical state. In other words,

we could describe every Cooper pair using the same wave function $\psi(\boldsymbol{x}, t)$. This is the macroscopic view of superconductivity!

Let us now write this wave function (which is equivalent to Ginzburg-Landau theory's order parameter) in the form which separates the absolute value and the phase of a complex valued function

$$\psi(\boldsymbol{x}, t) = \sqrt{\rho(t, \boldsymbol{x})} e^{i\delta(t, \boldsymbol{x})}, \tag{2.1}$$

assuming that $\rho(t, \boldsymbol{x}) > 0$. We are now free to choose any normalization one wants, but because we are dealing with a macroscopic number of bosons, $\rho(t, \boldsymbol{x})$ is clearly proportional to the pair density. We can therefore lock the normalization and identify that $\rho(\boldsymbol{x}, t)$ is the pair density. Normally the phase of a wave function has no effect on anything, but now the situation is different. Using the probability current of a wave function (which is proportional to the electrical current in this case) one obtains the coordinate dependence of the phase

$$\hbar \nabla \delta(t, \boldsymbol{x}) = m\boldsymbol{v} - 2e\mathbf{A}. \tag{2.2}$$

Here $\mathbf{A}$ is the vector potential of the system, $\boldsymbol{v}$ is the velocity of Cooper pairs and m is some effective mass of one Cooper pair. If we assume that the vector potential can't penetrate into the superconductor, like in the Meissner effect, deep inside the leads the derivate of the phase is proportional to the effective momentum of a Cooper pair and therefore to the supercurrent also. If this current is vanishing, the phase has the same value everywhere in the superconductor!

2.2 Classical Josephson Effect

When two superconductors are brought close together but are coupled only by a weak link (in this case a thin insulator), new effects can arise. This is because the probability amplitudes of Cooper pairs at the different sides of the insulator will couple to each other and start to oscillate. Similar effects are discussed in quantum mechanics quite often and they can be pictured quite simply. In figure 2.1 we introduce a voltage biased Josephson junction, it consist of two superconductors that are separated by a thin insulator and are attached to an ideal voltage source.

Let us assume that there is no magnetic field, the junction is symmetrical and no quasiparticles are present (that means no "normal electrons" are contributing to the system, all electrons are bounded). If the insulator is too thick, the states at the different sides of the insulator do not interact and nothing happens. If the insulator is thin, but not too thin, the probability amplitudes can interact with each other slighty. The system can be described by two coupled differential equations for the probability amplitudes [5, 9] at

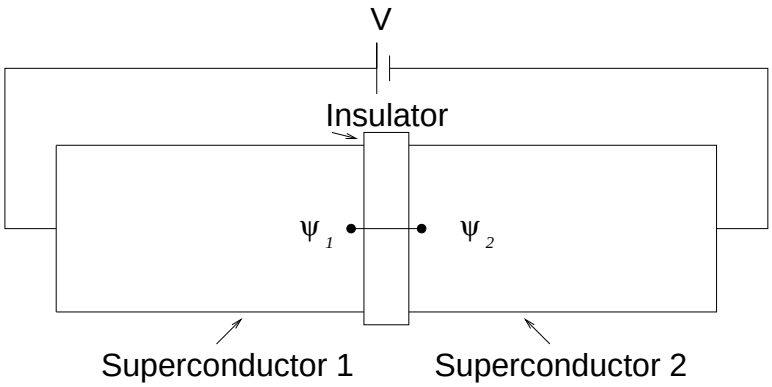

Figure 2.1: A voltage biased Josephson junction. The probability amplitudes ψ_i of Cooper pairs couple to each other and start to oscillate.

the points opposite sides of the junction, as drawn in figure 2.1. We have

$$i\hbar\frac{\partial\psi_1}{\partial t} = -eV\psi_1 + K\psi_2 \tag{2.3}$$

$$i\hbar\frac{\partial\psi_2}{\partial t} = eV\psi_2 + K\psi_1, \tag{2.4}$$

where K is certain coupling constant depending on the materials of the superconductors and the thickness of the insulator. Making the change of variables as in equation (2.1), taking into account the voltage source and a background charge ρ_0 of ions, one arrives after some algebra into two basic equations describing the Josephson effect

$$I_s = I_c \sin(\varphi) \tag{2.5}$$

$$\dot{\varphi} = \frac{2eV}{\hbar}. \tag{2.6}$$

I_s is the Josephson (super)current through the system and φ is the phase difference across the junction, defined as

$$\varphi = \delta_1 - \delta_2. \tag{2.7}$$

The time dependence in equation (2.6) is a result of an energy difference when a Cooper pair lies at the different sides of the junction. I_c is called the critical current and can be presented in the form

$$I_c = \frac{4eAK}{\hbar}\rho_0^*, \tag{2.8}$$

where A is the cross sectional area of the electrodes and ρ_0 is replaced by ρ_0^* which only differ in dimensions, $[\rho_0] = \frac{1}{m^3}$, $[\rho_0^*] = \frac{1}{m^2}$. I_c lies normally in the range of a microampere to milliampere, depending on a situation.

Notice that the macroscopic phases are now "locked" to each other unlike in the totally noninteracting case, where the idea of the phase difference is unsound.

Using the microscopic theory of superconductivity to the Josephson junction geometry, Ambegaokar and Baratoff worked out an exact result for the critical current [10] as a function of the BCS gap function $\Delta(T)$ (which describes the energy needed to excite an electron from the BCS ground state) and the normal state (not superconducting) resistance R_n. When $T = 0$ this can be written in the form

$$I_c = \frac{\pi \Delta(0)}{2eR_n}. \tag{2.9}$$

Equations (2.5) and (2.6) can now be easily solved to obtain the behaviour of the system as a function of time. Assuming that the voltage V between the superconductors is a constant we have

$$I_s = I_c \sin\left(\frac{2eV}{\hbar}t + c\right), \tag{2.10}$$

where c is an arbitrary constant resulting from the integration of equation (2.6). If now $V = 0$, we have a dc-current, even if there's an insulator between the conductors. The current depends sinusoidally on the constant c, it can have any value between $[-I_c, I_c]$. The phenomenon is called the dc-Josephson effect. If $V \neq 0$, the phase difference starts to travel as a function of time. This results in an oscillating supercurrent with an angular frequency $\frac{\hbar}{2eV}$ and an amplitude I_c over the insulator, so the net current integrated over time vanishes. This is called the ac-Josephson effect. We see that the Josephson junction behaves just the opposite than an ohmic resistor. If a nonzero voltage is applied, no net current is obtained. If a zero voltage is applied, a current flows through the system.

2.3 The Josephson Coupling Energy

In further analysis, the Josephson effect has to be described by a Hamiltonian formalism. This is crucial for example when going to the quantum mechanical treatment of the phenomenon. To do this, we have to find an energy which is released when the superconductors are brought close together, the Josephson potential energy. This can be deduced by considering the energy exchange between the junction and the voltage source when $V \neq 0$.

If there's a current I over a constant voltage V and it lasts time dt, the voltage source does the work $IV\,dt$. This energy has to be absorded in the

Josephson potential energy. The work done between the times t_0 and t is

$$\begin{aligned} W(t) &= \int_{t_0}^{t} I_s V dt' = \int_{t_0}^{t} I_c \sin\left(\frac{2eVt'}{\hbar} + c\right) V dt' \\ &= -\frac{\hbar}{2e} I_c \cos\left(\frac{2eV}{h}t + c\right) + \frac{h}{2e} I_c \cos\left(\frac{2eV}{h}t_0 + c\right) \\ &= -E_j \cos(\varphi) + \text{constant}, \end{aligned} \tag{2.11}$$

where we have introduced the Josephson coupling energy

$$E_j = \frac{h}{2e} I_c. \tag{2.12}$$

The constant in (2.11) is not important, it just shifts the zero point of energy. We can set it to zero and define

$$U = -E_j \cos(\varphi), \tag{2.13}$$

as the Josephson potential energy.

2.4 The Capasitance and Inductance of the Josephson Junction

In the last sections we assumed that there is a potential difference between the superconductors. This is possible if there's a charge gathered at the ends of the leads. Therefore, the Josephson junction can be seen as a capasitor whose charge is described by the capasitance C

$$Q = CV. \tag{2.14}$$

The capasitor stores a Coulomb energy in the junction region which can be written in the form

$$E_Q = \frac{Q^2}{2C}. \tag{2.15}$$

This is called the Josephson kinetic energy. A charging energy is the fundamental unit of electric processes present in Josephson junctions. It is defined as the energy when there's effectively one electron charge in the electrodes

$$E_c = \frac{e^2}{2C}. \tag{2.16}$$

We can now relax the assumption of a voltage bias and study a system which has no contact to the outer world. Its dynamics are then controlled by the Josephson potential energy and the Josephson kinetic energy. We write the Hamiltonian as a sum of these two terms

$$H = -E_j \cos\varphi + \frac{Q^2}{2C}. \tag{2.17}$$

If one assumes that φ is localised nearby one of the local minima of $-E_j \cos\varphi$ potential (equivalent to that $I_s \ll I_c$ for all times), one can approximate the cosine-function by the first two terms of its power series. We have

$$H = \frac{E_j}{2}\varphi^2 + \frac{Q^2}{2C} + \text{constant}. \tag{2.18}$$

We will again forget the constant. Equation (2.18) can be written in a more familiar form using the approximation $I = I_c \sin(\varphi) \approx I_c\varphi$

$$H = \frac{\hbar^2}{8E_j e^2} I^2 + \frac{Q^2}{2C} = \frac{L}{2} I^2 + \frac{Q^2}{2C}, \tag{2.19}$$

where we have introduced L, the inductance of the Josephson junction

$$L = \frac{\hbar^2}{4e^2 E_j}. \tag{2.20}$$

The Hamiltonian (2.19) is the same as for an LC-oscillator, familiar from alternating current circuits, so its solution is a harmonic oscillation around the mean value. The phase difference is therefore oscillating around the local minimum of the Josephson potential energy with an angular frequency ω_p, called the plasma frequency of the Josephson junction

$$\omega_p = \sqrt{\frac{1}{LC}} = \frac{1}{\hbar}\sqrt{8E_j E_c}. \tag{2.21}$$

2.5 Superconducting Quantum Interference Device

New effects will occur when a magnetic field is applied to the Josephson junction area. We will now concentrate on the effects which will come into existence in a superconducting ring interrupted by two Josephson junctions, shown in figure 2.2. The system is called a SQUID (Superconducting QUantum Interference Device).

We know that the magnetic field "shifts" the phases of the probability amplitudes in a path integral description of quantum mechanics. As a result, it turns out that instead of φ one has to use so-called gauge-invariant phase difference to describe the tunneling across the insulator. It is defined as

$$\phi_g = \varphi - \frac{2\pi}{\Phi_0}\int_1^2 \mathbf{A}\cdot d\boldsymbol{s}, \tag{2.22}$$

where the integration path is between the points at the opposite sides of the insulator (as shown in figure 2.1) and $\phi_0 = \frac{h}{2e}$ is the flux quantum. The Josephson current is now

$$I_s = I_c \sin(\phi_g). \tag{2.23}$$

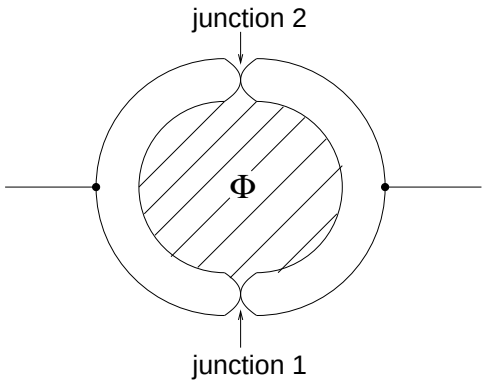

Figure 2.2: Superconducting QUantum Interference Device. Two Josephson junctions interrupt a superconducting ring.

Let us assume that the leads are thick enough, so the magnetic field can't penetrate inside the electrodes. However, because of this special situation, the vector potential $\mathbf{A}$ doesn't have to vanish inside them. If there were no Josephson junctions in the superconducting ring, the magnetic flux enclosed by the ring would be quantized and a basic quantum would be Φ_0. With the help of equation (2.2) and assuming that $\boldsymbol{v}$ is vanishing we obtain [4]

$$\mathbf{A} = -\frac{\Phi_0}{2\pi}\nabla\delta, \tag{2.24}$$

inside the electrodes. Thus

$$\Phi = \oint \mathbf{A}\cdot d\boldsymbol{s} = -\frac{\Phi_0}{2\pi}\int_{\text{electrodes}} \nabla\delta\cdot d\boldsymbol{s} + \int_{\text{links}} \mathbf{A}\cdot d\boldsymbol{s}. \tag{2.25}$$

The integral across the electrodes gives the phase difference of one loop (which must be $n2\pi$, where n is an integer), minus the finite phase differences across the weak links

$$\int_{\text{electrodes}} \nabla\delta\cdot ds = n2\pi + \varphi_1 - \varphi_2. \tag{2.26}$$

Combining this with equations (2.22) and (2.25) we obtain

$$\phi_{g2} - \phi_{g1} = \frac{2\pi\Phi}{\Phi_0} + n2\pi, \tag{2.27}$$

where ϕ_{g1} are ϕ_{g2} are the gauge-invariant phase differences across the junctions 1 and 2. Unlike in the case of the superconducting ring, the flux can have any value and therefore is not quantized but the phase differences are suffering, they are not independent. If we now calculate the current, we see

that the contributions through the different junctions are partly cancelling each other. Especially if $I_{c1} = I_{c2}$ then

$$I = 2I_c \cos\left(\frac{2\pi\Phi}{\Phi_0}\right) \sin(\phi_g). \tag{2.28}$$

This shows that the SQUID can be seen as a single Josephson junction with an adjustable coupling energy. Because of this remarkable feature, SQUIDs have had a huge amount of applications in building very sensitive magnetic field detectors and, for example, in macroscopic quantum physics. It is argued that the SQUID is the most important application of superconductivity so far.

In future, if dealing with the magnetic field, we will simply mark ϕ_g by φ to keep the equations simple and in harmony with the literature. To complete the analogy with a single junction case, we would like to know the effective capasitance of the SQUID. It is obtained by considering the SQUID as two capasitors in a parallel configuration

$$C = C_1 + C_2. \tag{2.29}$$

Especially if $C_1 = C_2$ (and there is no magnetic field), then the SQUID has douple the coupling energy and the capasitance of the single junction. This results in that the charging energy is half of the original and thus the plasma frequency in equation (2.21) stays constant.

2.6 The RCSJ-Model

So far, we have considered Josephson junctions which are voltage biased or not biased at all. Also no quasiparticle current is included yet. However, in practical experimental situations a small quasiparticle current is always present and it will introduce a dissipation into our system. We will first include this effect in a situation where we have a current bias. This leads to an analogous differential equation as for a particle in certain effective potential field. Thinking the Josephson junction as a single particle, will help us to understand its dynamics. It is called the Resistively and Capasitively Shunted Junction model, shortly the RCSJ-model.

The key idea in the RCSJ-model is to describe the Josephson junction with an equivalent model which contains a capasitor, a resistor and the Josephson supercurrent in a parallel configuration, as shown in figure 2.3. Because the charge is conserved, an input current must be in a balance with the current through the junction. There are three channels which are contributing to it. This leads to the differential equation

$$I = I_c \sin(\varphi) + GV + C\frac{dV}{dt}, \tag{2.30}$$

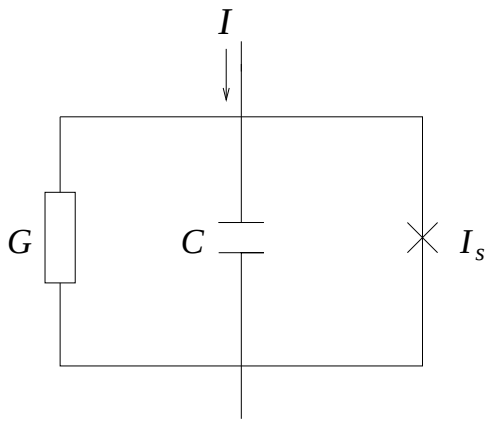

Figure 2.3: The RCSJ-model of the Josephson junction. The resistor is described by its conductance G.

where I is the input current and G is the conductance of the quasiparticle current. Using equation (2.6) we can eliminate the voltage by the phase difference and obtain the second order differential equation

$$C\left(\frac{\hbar}{2e}\right)^2 \ddot{\varphi} = \frac{\hbar}{2e} I - \left(\frac{\hbar}{2e}\right)^2 G\dot{\varphi} - E_j \sin(\varphi). \tag{2.31}$$

The differential equation is the same than for a particle of mass $C(\frac{\hbar}{2e})^2$ moving along φ-axis in an effective potential

$$U(\varphi) = -E_j \cos(\varphi) - \frac{\hbar}{2e} I\varphi, \tag{2.32}$$

with a friction factor $\left(\frac{\hbar}{2e}\right)^2 G$. A useful quantity describing the damping is the quality factor D defined as

$$D = \frac{C}{G}\omega_p. \tag{2.33}$$

The effective potential contains the Josephson potential energy but it also contains the input current which just tilts the potential. If the friction and the current are vanishing, we obtain harmonic oscillations at the bottom of some local minimum, as derived in section 2.4 (supposing that the particle hasn't got enough energy to escape from the local minimum). If a low friction is applied ($D \gg 1$), we obtain underdamped oscillations: after some period of time (long compared to the plasma oscillations) the particle stops at the bottom of the local minimum. If the potential is tilted (increasing the input current) and it has the energy to "climb" at the local maximum of the potential, the particle can escape without never stopping. Its energy is dissipated but the particle obtains it back from the tilt of the effective

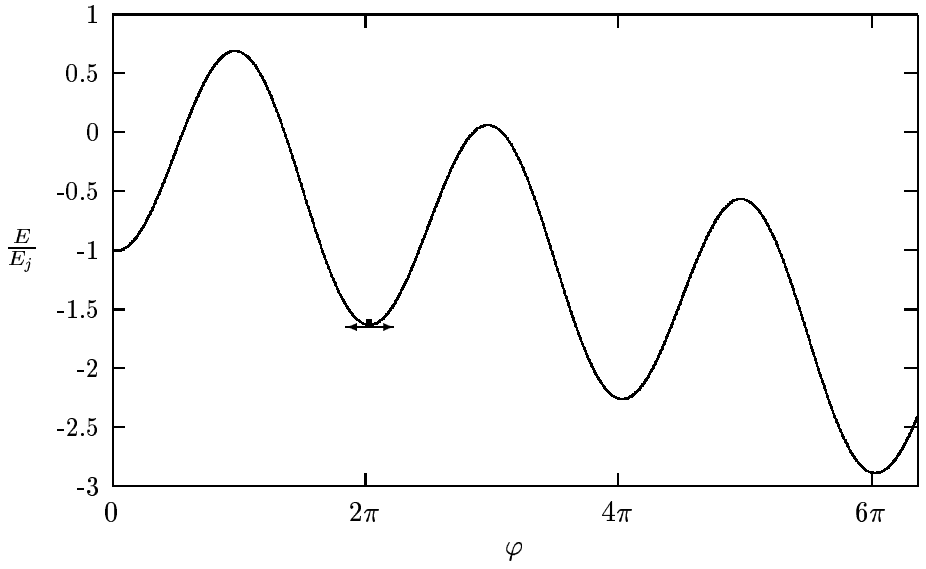

Figure 2.4: The particle is localized at the bottom of the tilted potential when $I = \frac{1}{10}I$. The local minimum isn't exactly 2π.

potential, supposing that the friction is not too large (or the tilt too low). This corresponds to an oscillating supercurrent with a presence of a small quasiparticle current. If the friction is too large (for example overdamped junction $D \ll 1$), the particle jamms at the local minimum of the effective potential and finally stopps. This is not the minimum of the Josephson potential because of the tilt. As a result, there is a supercurrent flowing through the junction, which exactly cancels the current bias. Situation is shown in figure 2.4.

One should note that in the real situation the quasiparticle conductance is not necessary ohmic, its a function of a voltage $G = G(V)$. It's ohmic in the region $V > \frac{2\Delta(T)}{e}$ when the corresponding resistance approaches the normal state resistance. The voltage can now easily break Cooper pairs to obtain the quasiparticle current. However, when dealing in the undergap region ($V < \frac{2\Delta(T)}{e}$), the conductance drops dramatically because thermal activitation is needed for the quasiparticle tunneling to occur. In this region the conductance is not ohmic and lowers expenentially when lowering the temperature. In our situations of interest the leads are made of aluminum and the gap function of them has the value $\approx 200\ \mu eV$ at low temperatures. This defines the undergap region to be at $V \leq 400\ \mu V$.

In the RCSJ model we clearly see the ultimate coherence of the superconductors. Despite the fact that we have a macroscopic number of electrons participating in the junction's dynamics, it behaves as it would be a single

particle. Cooper pairs act as an entity, not statistically like fermions. This is the key fact why macroscopic quantum phenomena is possible to achieve in the Josephson junction based systems.

Chapter 3

Current Voltage Peaks in Classical Many Josephson Junction Systems

The purpose of this chapter is to study current-voltage peaks appearing in voltage biased many Josephson junction systems. Especially we are studying peaks in a situation where there are two classically behaving mesoscopic junctions with different Josephson coupling energies in series with the voltage source. Then in chapter 7 we compare the results with the theory of inelastic Cooper pair tunneling, which gives rise to similar peaks. We start by historical introduction of closely related topics, Shapiro and Fiske steps. Then later we write down the differential equations of dissipative two Josephson junction systems. After that we show the results of our numerical calculations for the current-voltage characteristics. Finally we extend the model to many Josephson junction systems.

3.1 Shapiro Steps

In 1962 it was discussed by Josephson [6] also that in the presence of microwaves, the Josephson current might be nonvanishing for special values of the dc-voltage. First detection of this was made by Shapiro [11] a year later in an experiment where a clear step structure was found in the dc $I-V$ curve. This was also an indirect detection of the ac-Josephson effect.

The Shapiro steps arise when a Josephson junction is biased by a rf-drive which has both the ac- and dc-components. Let us now analyze in detail, how this can be possible. We assume that we have an ideal voltage source and [4]

$$V(t) = V_0 + V_1 \cos(\omega_1 t). \tag{3.1}$$

With the help of equation (2.6), the phase difference across the junction can

be written in the form

$$\varphi(t) = c + \frac{2eV_0}{\hbar}t + \frac{2eV_1}{\hbar\omega_1}\sin(\omega_1 t), \tag{3.2}$$

where c is an arbitrary constant resulting from the integration. Assuming an ohmic conductance for quasiparticles, we can use equation (2.30) and have

$$\begin{aligned} I(t) = I_c \sin\left(c + \frac{2eV_0}{\hbar}t + \frac{2eV_1}{\hbar\omega_1}\sin(\omega_1 t)\right) \\ +G(V_0 + V_1\cos(\omega_1 t)) - CV_1\omega_1\sin(\omega_1 t). \end{aligned} \tag{3.3}$$

To get the observable current, we need to time average (3.3). The first term (which is the supercurrent) can be written with the help of Bessel functions J_n

$$I_s = I_c \sum (-1)^n J_n\left(\frac{2eV_1}{\hbar\omega_0}\right)\sin(c + \omega_0 t - n\omega_1 t), \tag{3.4}$$

where we have defined $\omega_0 = \frac{2eV_0}{\hbar}$. Timeaveraging (3.4) leads to a nonvanishing value only when V_0 has one of the Shapiro step values

$$V_0 = V_n = n\frac{\hbar\omega_1}{2e}. \tag{3.5}$$

As in the dc-Josephson effect, its value is sinusoidally dependent on the constant c. We see that the time average of the current (3.3) is distributed to values

$$GV_n - I_c J_n\left(\frac{2eV_1}{\hbar\omega_1}\right) \leq I \leq GV_n + I_c J_n\left(\frac{2eV_1}{\hbar\omega_1}\right). \tag{3.6}$$

To get it simple, the Shapiro steps are arising when the ac-Josephson effect is in harmony with the alternating voltage source. Their magnitude can be calculated with the help of Bessel functions. The name "step" becomes from the fact that when V is plotted as a funtion of I, one obtains a steplike $I - V$ structure.

Same kind of phenomena can occur even at a constant voltage bias if some internal cavity mode is present and it can interact with the Josephson current. In 1964 Fiske observed peaks which were interpreted as resonances with electromagnetic cavity modes in long Josephson junctions [12]. These can occur if the electromagnetic field can penetrate deep enough in the junction resulting an interaction with the Josephson current. As a result, steps are formed in the $I - V$ curve of the system as in the previous case.

Recently the Josephson effect was investigated in a situation where the insulating potential was coupled to a harmonic oscillator [13]. As a result, the Josephson ac-current coupled to these harmonic oscillations forming a step structure in the dc $I - V$ curve, similar as in the Shapiro effect. Investigations of such a systems are vital because of possible applications to nanoelectronics and quantum information processing.

3.2 Resonances in Many Josephson Junction Systems

We start now to seek Shapiro structures which come into existence in many Josephson junction systems. The phenomenon can occur if there are many junctions with different coupling energies in series with a dc-voltage source. Reconances don't need an alternating voltage or electromagnetic cavities present in the junction. Effectively one junction can act as the alternating voltage source to another, leading to a peak structure in the $I-V$ curve.

Dynamics for a voltage biased classical multijunction system are easily generalized from the case of a single junction introduced in chapter 2. The current through the i:th junction is

$$I_i = I_{ci}\sin(\varphi_i) + C_i\frac{dV_i}{dt} + G_iV_i, \tag{3.7}$$

where φ_i is the phase difference across the i:th junction and so on. The voltage source "locks" the phase difference φ_Σ over the whole system but the local phases can have arbitary values, within the limits that φ_Σ is as expected. The time dependences of the phase differences are as before

$$\dot{\varphi}_\Sigma = \frac{2eV}{\hbar} \tag{3.8}$$

$$\dot{\varphi}_i = \frac{2eV_i}{\hbar} \tag{3.9}$$

$$\varphi_\Sigma = \sum_i \varphi_i \tag{3.10}$$

$$V = \sum_i V_i. \tag{3.11}$$

Let us study a simple situation where there are two Josephson junctions in series with a voltage source. Let us assume that one junction has much larger Josephson coupling energy than the other. We call the little one a probe junction, the name will become clear in the later chapters. We assume also that the quasiparticle conductances vanish, $G_i = 0$. Using equations (3.7) and (3.9), we obtain the currents flowing through the junctions

$$I_{c1}\sin(\varphi_1) + C_1\frac{\hbar\ddot{\varphi}_1}{2e} = I_1 \tag{3.12}$$

$$I_{c2}\sin(\varphi_2) + C_2\frac{\hbar\ddot{\varphi}_2}{2e} = I_2. \tag{3.13}$$

We know that $I_1 = I_2 = I(t)$ because the charge doesn't disappear. These equations are actually two equations for the same phase difference, since under a voltage bias the phase differences are not independent, as seen from

equations (3.8) and (3.10). We can eliminate $I(t)$ by substracting equations (3.12-13) from each other and have

$$I_{c1}\sin(\varphi_1) + (C_1 + C_2)\frac{\hbar\ddot{\varphi}_1}{2e} - I_{c2}\sin\left(\frac{2eVt}{\hbar} + c - \varphi_1\right) = 0. \tag{3.14}$$

Solving the differential equation (3.14) and then using the relation (3.12) one can calculate the current as a function of the voltage and the constant c.

Let us now derive an approximate solution. We shall assume that the larger junction's phase difference is stucked at the bottom of its local minimum, as in figure 2.4. If there's a net current flowing, we could say that its mean position deviates from the bottom of the cosine-potential a little, as in the tilted washboard case. We assume that the mean position is φ_m and the little deviation from this is φ. Then equation (3.12) can be approximated in the form

$$I_{c1}\varphi + C_1\frac{\hbar\ddot{\varphi}}{2e} = I(t) - I_{c1}\varphi_m. \tag{3.15}$$

If $I_{c1} \gg I_{c2}$, the right hand side of equation (3.15) is assumed to be a small perturbation and will be set to be zero. Then the solution of equation (3.15) is harmonic and independent of φ_2 (which is not true!). So it can be written in the form

$$\varphi = a\sin(\omega_p t + b), \tag{3.16}$$

where ω_p is the plasma frequency of the larger junction and a and b are some "arbitrary" constants (of cource $a \ll 1$). As a result, φ_1 oscillates around its mean position, acting as an effective rf voltage source to the smaller junction. The time dependence of φ_2 can be written in the form

$$\dot{\varphi}_2 = \frac{2eV}{\hbar} - \dot{\varphi}_1 = \frac{2eV_0}{\hbar} - V_1\cos(\omega_p t + b), \tag{3.17}$$

where we have identified $a\omega_p = V_1$ and $V = V_0$, showing the equivalence for the Shapiro step case. Now the calculaction continues in a similiar way as done in the previous section, resulting steps in the $I - V$ curve.

We eliminated the other junction to act as an effective ac-voltage source of an angular frequency ω_p. The approximation clearly gives raise to Shapiro like steps which are spaced by $\frac{\hbar\omega_p}{2e}$ in the voltage axis, but we cannot know anything about the magnitudes of the resonant currents because the crucial parameter a is undetermined. Also the "relative" phase difference constant between the junctions, which gives raise to the step-like behaviour, is assumed to be arbitrary (corresponds to the constant c in the Shapiro step case) and this might not be true for this case. Actually, in the same fashion

as done before, it could be argued that the asymmetric two Josephson junction system is analogous to a damped harmonic oscillator under a sinusoidal external force. The larger junction forms the harmonic oscillator and the smaller junction gives rise to almost sinusoidal force. In this model, there will be a resonance at $2eV = \hbar\omega_p$ but with no dependence of the "Shapiro constant" c to the current and no higher resonances are present.

From numerical calculations we obtain that the real situation for the Josephson junctions is somewhere between these two cases. To obtain a current when $V \neq 0$, we have to introduce also a dissipation mechanism (the reason for this will be discussed in section 3.3). At $V = 0$ the phase difference relaxes to the bottom of the Josephson potential, no dynamics are present. The current depends sinusoidally on the constant c, just like in the dc-Josephson effect. When $V \neq 0$, the c dependence weakens and finally disappears. Because of the quasiparticle tunneling, the "noise" current rises linearly as a function of the voltage. At $2eV \approx \hbar\omega_p$ there is a clear resonance. However, the current has two solutions for the same voltage, depending from which direction we are coming to the region. This means that the solution is hysteretic. If we replace the larger junction's potential energy by harmonic oscillator approximation, the hysteresis disappears and the peak is almost a Lorenzian curve, as shown in figure 3.1. The hysteretic behaviour is discussed more detailed in section 3.6. Parameters for the calculation were partly taken from an experinment made by R. Lindell *et al.* [14] for mesoscopic Josephson junctions.

3.3 Energetic Point of View

One could ask how the Shapiro steps are even possible to appear because the situation in section 3.1 had no dissipation. We have a net current when there's a voltage applied across the system and no dissipation is present. Where does the energy go? The answer is simple: the alternating voltage takes care of the energy conservation. When a resonance occurs, the ac-source absorbs the energy which the dc voltage source is feeding. The mean voltage is still V but the current won't vanish.

Thinking of this one sees a difference for the two Josephson junction system. In section 3.2 there was a dc-voltage applied over the whole system and still a current was obtained. Our system absorbs the energy as in the Shapiro step-case, but it has to dissipate it also (for example by quasiparticle tunneling). Otherwise its oscillation amplitude would start to rise continuously (which was forgotten in the heuristic approach) and no net current would be finally obtained. This shows that to obtain resonances in the voltage biased many Josephson junction system, also a dissipation mechanism has to be taken into account.

Figure (3.1a)

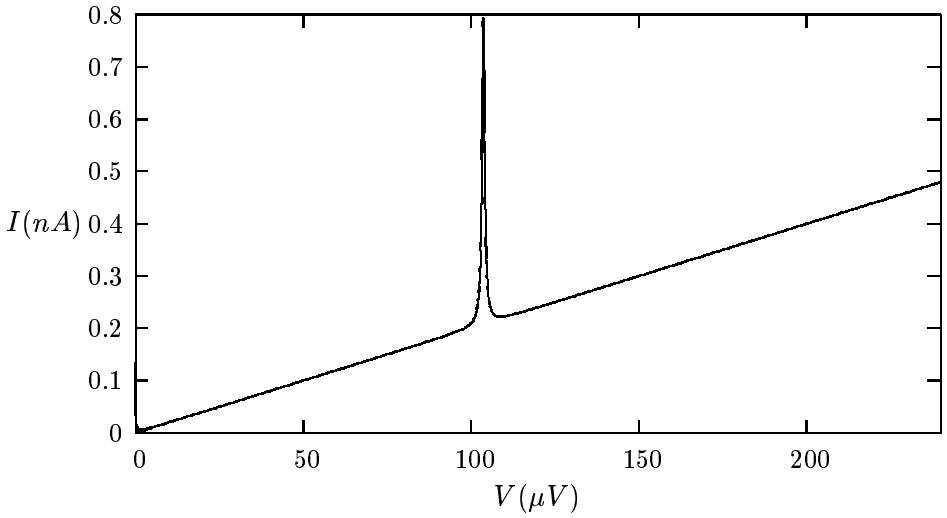

Figure (3.1b)

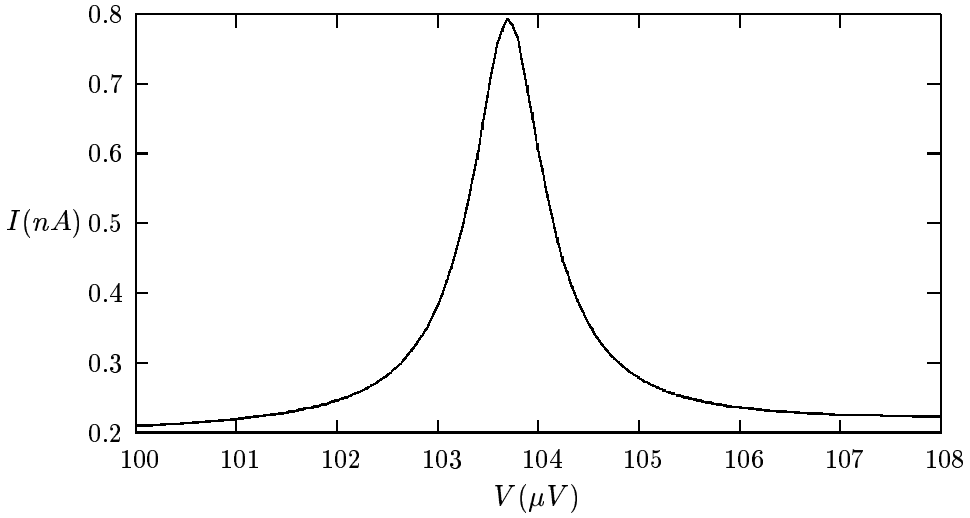

Figure 3.1: The $I-V$ curve of the parabolic approximation. The main parameters in the calculation were $c=\frac{\pi}{2}$, $G_1=20\,\mu\frac{1}{\Omega}$, $G_2=2\,\mu\frac{1}{\Omega}$, $\hbar\omega_p=213.8$ μeV. The current is increasing continuously because of the quasiparticle current. As seen from the figure 3.1b, the resonance is a Lorenzian peak and locates near $\frac{\hbar\omega_p}{2e}=106.9$ μV but not exactly there. Its location is determined by an effective plasma frequency of the system $\omega_e\approx 2\times 103.7$ μeV (we will use this notation for the plasma frequencies because then the positions of the peaks are easy to see just by eliminating the factors 2 and e), defined as using capasitance $C_\Sigma=C_1+C_2$ instead of C_1 in (2.21). This frequency is introduced in chapter 6.

3.4 Differential Equations for the High Frequency Limit

When performing an experiment, we have to attach current or voltage leads to the junction. Even if there isn't any resistance in the dc-current flow of superconductors, it will be present at high frequency prosesses and of order $R \approx 50 - 100\ \Omega$ when $\omega \sim 10^{11}\ \frac{1}{s}$ [30]. For large junctions and normal voltages the quasiparticle resistance is smaller than this and the leads won't give any extra contribution to the system (now the effective dissipation source is a parallel configuratation of the lead and the quasiparticle resistance). However, because we are dealing with small junctions (implying that $R_n \geq k\Omega$) and in the undergap region this effect shouldn't be vanishing, as a matter of fact it should be the dominant dissipation mechanism. We will therefore add a resistor to our system to describe the effect of the leads. We will also include the quasiparticle current and keep the assumption of a voltage bias, as shown in figure 3.2. To be sure that these two resistance sources are not mixed up, we have used throughout the thesis a conductance to describe the quasiparticle current and a resistance to describe the high frequency resistance of the leads.

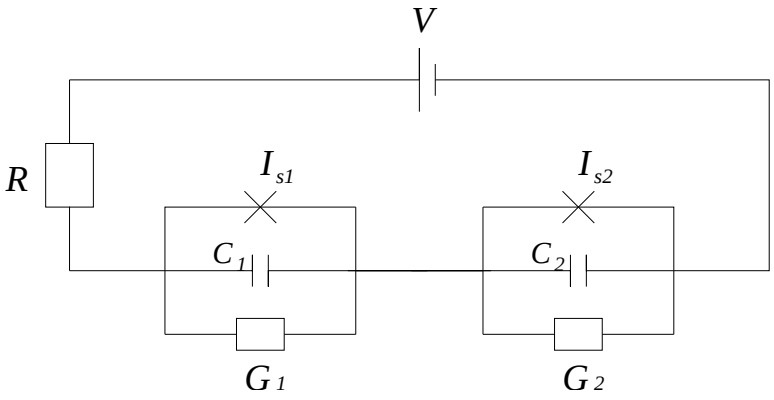

Figure 3.2: A model for dissipative two Josephson junction system. The resistor in series corresponds to the high frequency resistance of the leads and the conductors in parallel correspond to the quasiparticle currents.

We start by writing three coupled differential equations for the current through the system, corresponding to two Josephson junctions (equation

(3.7)) and the resistor (Ohm's law)

$$I_{c1}\sin(\varphi_1) + G_1\frac{\hbar\dot{\varphi}_1}{2e} + C_1\frac{\hbar\ddot{\varphi}_1}{2e} = I(t) \tag{3.18}$$

$$I_{c2}\sin(\varphi_2) + G_2\frac{\hbar\dot{\varphi}_2}{2e} + C_2\frac{\hbar\ddot{\varphi}_2}{2e} = I(t) \tag{3.19}$$

$$\frac{V_R}{R} = I(t). \tag{3.20}$$

Only two of them are independent which can be seen by transforming (3.20) with the help of relation $V = V_1 + V_2 + V_R$ into the form

$$\frac{1}{R}(V - V_1 - V_2) = \frac{\hbar}{2eR}\left(\frac{2eV}{\hbar} - \dot{\varphi}_1 - \dot{\varphi}_2\right) = I(t). \tag{3.21}$$

Putting the left hand side of equation (3.21) into the right hand sides of equations (3.18) and (3.19) we obtain

$$\ddot{\varphi}_1 = \frac{1}{C_1}\left[\frac{2eV}{\hbar R} - \left(\frac{2e}{\hbar}\right)^2 E_1\sin(\varphi_1) - \dot{\varphi}_1\left(\frac{1}{R} + G_1\right) - \frac{\dot{\varphi}_2}{R}\right] \tag{3.22}$$

$$\ddot{\varphi}_2 = \frac{1}{C_2}\left[\frac{2eV}{\hbar R} - \left(\frac{2e}{\hbar}\right)^2 E_2\sin(\varphi_2) - \dot{\varphi}_2\left(\frac{1}{R} + G_2\right) - \frac{\dot{\varphi}_1}{R}\right]. \tag{3.23}$$

These are the two coupled differential equations which describe the dynamics of a classical voltage biased two Josephson junction system. To solve them we have to use numerical methods.

3.5 The Harmonic Oscillator Approximation

As mentioned before, calculating the current of two Josephson junction system with $E_1 \gg E_2$ is very analogous to measuring an amplitude of a periodically forced harmonic oscillator with damping. This is because firstly, the Josephson potential energy of the larger junction is close to a harmonic potential for the relevant values of φ_1, and secondly, measuring the amplitude of damped oscillations with certain forcing frequency is equivalent to finding the amplitude of a current as a function of the dc-voltage.

In harmonic oscillator approximation we describe the larger Josephson junction's potential energy purely by a harmonic potential (which means replacing $\sin(\varphi_1)$ by φ_1 in equations (3.18) and (3.22)). In the limit $E_1 \gg E_2$ the "drive force" is almost sinusoidal for large voltages because the smaller junction's phase difference is moving with a high velocity in its Josephson potential curve, resulting in an almost sinusoidal energy oscillation. Under a sinusoidal force, the damped oscillator's energy dissipation as a function of the driving frequency is a Lorenzian curve. So we expect that the (net) current as a function of the voltage is more or less a Lorenzian curve.

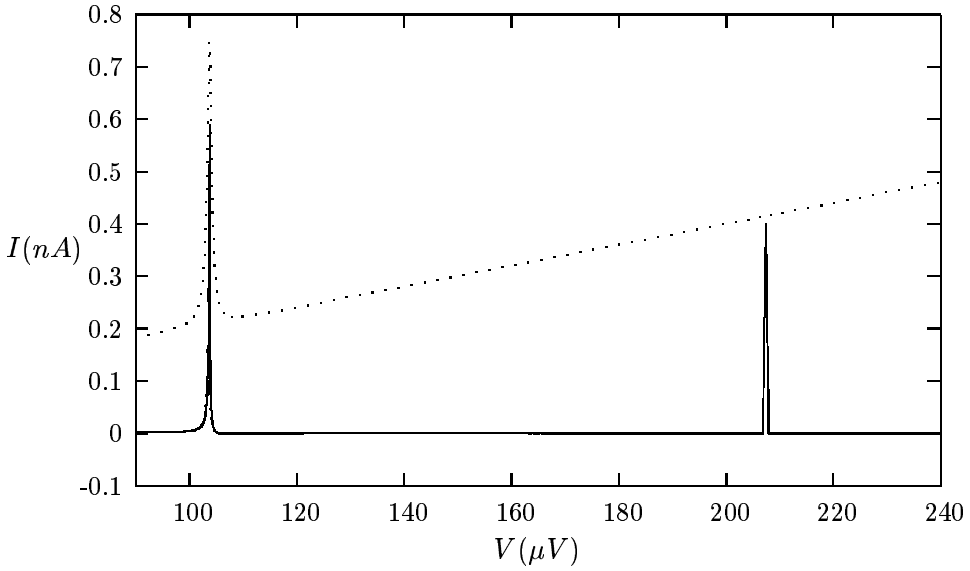

Figure 3.3: The I-V characteristics of the harmonic oscillator approximation for two different quasiparticle conductances. A solid line corresponds to $R = 100\Omega$, $G_1 = G_2 = 0$ and a dotted curve to $G_1 = 20\mu\frac{1}{\Omega}, G_2 = 2\mu\frac{1}{\Omega}$. The second peak (the first harmonic) disappears smoothly when increasing the quasiparticle conductance. The peaks are located at $\frac{\hbar\omega_e}{2e}$ and $\frac{\hbar\omega_e}{e}$ and no resonances are found for higher voltages.

Numerical results for the $I - V$ characteristics are plotted in figure 3.3 for two different quasiparticle conductances. We are only interested of the high frequency area $V \gg 0$ because the model doesn't apply for $V \approx 0$. Parameters of the Josephson junctions are the same as before.

As we see, there are clearly two resonances. The quasiparticle current increases linearly as a function of the voltage which gives a rise to a constantly increasing current. The magnitude of the second reconance (we can call this the first harmonic) is of the same order than the first one when $G_i = 0$. In figure (3.4) we plot the $I - V$ characteristics of the first resonance (usually called the fundamental resonance) for different resistances. As we see, the curve is almost Lorenzian and becomes wider when the resistance is increased, as expected. However, the maximum of the resonance starts to shift to the right for higher resistances and the peaks become hysteretic for lower resistances.

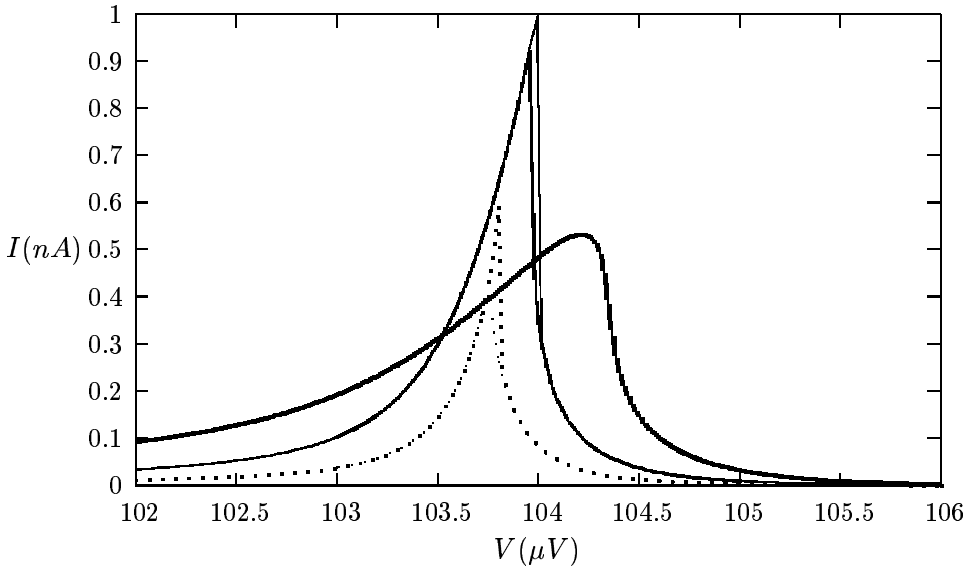

Figure 3.4: The I-V characteristics of the first resonance for different resistances. The solid curves whose maximum is at 104.25 μV corresponds to $R = 1\ k\Omega$. Its shape is asymmetric and tilted to right. The solid curves whose maxima are near 104 μV correnpond to $R = 300\ \Omega$. The solution is multivalued depending on from which side we are approaching the resonance region. The dotted curves correspond to $R = 100\ \Omega$ and they also manifest a slight hysteresis. For all curves $G_1 = G_2 = 0$.

3.6 Effect of Anharmonic Oscillations

It is well known that adding small higher order (anharmonic) terms to a damped harmonic oscillator under a periodic force, the fundamental resonances start to shift [15]. As a concequence of this, if the higher order components are strong enough, there might be two possible solutions for the same voltage. Also multiples of the fundamental resonances can appear (which already happened in the previous situation as the existence of the second peak). When we will describe the larger junction's potential energy with its original form, $-E_1 \cos(\varphi_1)$ the shape of the resonances will greatly change from the previous situation. This can be understood qualitatively by thinking the power series of the cosine potential. In the resonance region, the amplitude of the oscillation is larger than in the non-resonance case and also the higher order terms of the power series will be signifigant. How significant, depends of course on the specific parameters of the junctions. As a result, this gives rise to anharmonic terms and hysteresis.

Since there was a second resonance already in the harmonic oscillator approximation, one can deduce that the "drive force" introduces some anharmonic terms also. This is natural since the movement of φ_1 affects the movement of φ_2 and therefore the drive force has a small dependence of φ_1.

In figure 3.5 is shown the $I-V$ characteristics calculated using equations (3.22) and (3.23). Everywhere else than in the resonance region the $I-V$ curves for different conductances are similar than in the harmonic oscillator approximation. When arriving from the left side to the resonance, the solution jumps discontinuously to higher value and then smoothly lowers when increasing the voltage. Prosess is a mirror image of the one seen in figure 3.4. Shift of the right side solution is huge and it disappears (or is not found) for higher conductances. Keeping the plasma frequency constant but changing the other variables of the junction so that the harmonic approximation is more valid, we can decrease the hysteresis in the numerical modelling, just as expected. No resonances are found for higher voltages.

For comparison, the numerical results when not taking the lead resistance into account (the model in section 3.2) show that the $I-V$ curves for different conductances are similiar than when arriving from the left side in figure 3.5. Two resonances are found but the magnitude of the latter is very small. Similar multi-valuedness is observed when arriving from the right side but it lasts only for a very short distance. Probably this is because of its weak nature to crash into the lower current solution.

3.7 Many Josephson junction systems

Coupled differential equations (3.22) and (3.23) can be easily generalized to many Josephson junction systems. Looking at the procedure done in (3.18-

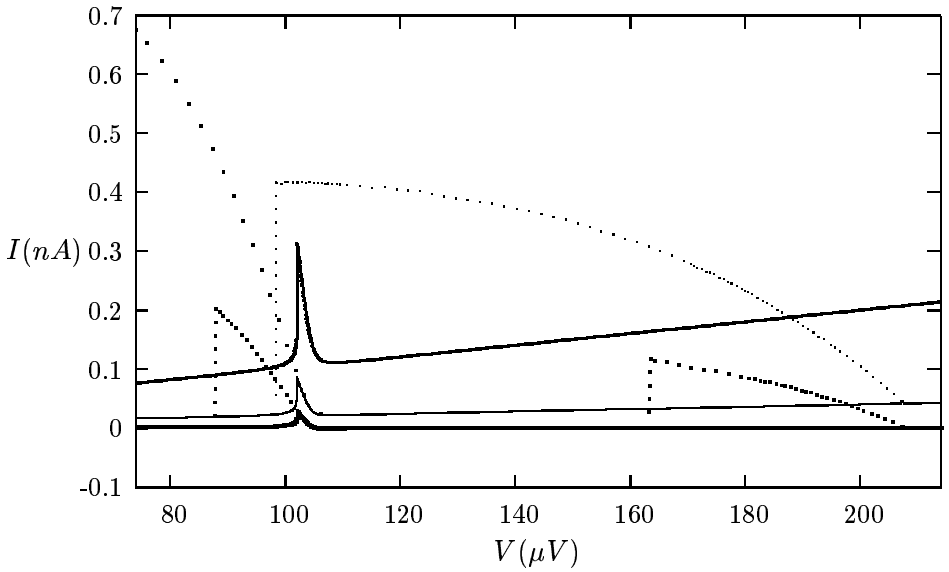

Figure 3.5: The I-V characteristics of the dissipative two Josephson junction system for different quasiparticle conductances. Solid lines correspond to arriving from the left to the resonances and the dotted curves correspond to arriving from the right. When $G_1 = G_2 = 0$ (curve is at the "bottom" of the plot) the resonances are "streched" for huge distances when arriving from the right to left. Situation $G_1 = 2\ \mu\frac{1}{\Omega}$, $G_2 = 0.2\ \mu\frac{1}{\Omega}$ is even more wild, the hysteresis of the second resonance lasts beyond the first one. Three solutions are possible in the region $V \approx \hbar\omega_c$ and the first resonance streches all the way to 60 μV. The hysteresis disappears for $G_1 = 1\ \mu\frac{1}{\Omega}$, $G_2 = 10\ \mu\frac{1}{\Omega}$ (the highest solid curve). Peaks start from the positions $\hbar\omega_e$ and $2\hbar\omega_e$ as in the previous cases.

23) one can deduce that the differential equation for the i:th phase difference in n Josephson junction system is

$$\ddot{\varphi}_i = \frac{1}{C_i}\left[\frac{2eV}{\hbar R} - \left(\frac{2e}{\hbar}\right)^2 E_i \sin(\varphi_i) - G_i\dot{\varphi}_i - \frac{1}{R}\sum_{j=1}^{n}\dot{\varphi}_j\right]. \qquad (3.24)$$

As a result, we have n coupled second order differential equations which have to be solved by numerical methods. A special case of this, using two large junctions in series with the small one, is solved numerically in chapter 7.

As a summary, we have clearly shown that an asymmetric situation in a voltage biased classical many Josephson junction system gives rise to peaks in the current voltage-characteristics of the system. The peaks are not step-like as in the Shapiro step case, they are mostly unique functions of the voltage. But also many solutions for the same voltage are possible resulting from the hysteresis of the solutions. The model is only an approximation of the practical behaviour of a real system, the conductances might not be really ohmic and correct values for them are hard to deduce. The effect of the high frequency lead resistance for small Josephson junctions might also be a little different. The overall behaviour however should be close to the one described above.

Chapter 4

Secondary Quantum Macroscopic Effects

In this chapter we will discuss the quantum mechanical treatment of the Josephson effect. In the treatment we will replace all "classical" parameters, like the phase difference across the junction, by quantum mechanical operators and solve the eigenfunctions of the relevant Hamiltonian. The new effects that arise are then called the "secondary" quantum macroscopic effects because the "primary" macroscopic quantum effect is the classical Josephson phenomenon itself. At first we will study when these secondary effects can be significant. After solving the Hamiltonian, discussion of a discrete charge transfer is needed. With the help of that we explain the Bloch-wave oscillations for small Josephson junctions under a weak current bias. Finally we will discuss the experimental and the theoretical disagreements of the Josephson coupling energies for mesoscopic Josephson junctions. The chapter is based on similar discussions made in Refs. [32, 30, 16, 26].

4.1 Insufficiency of the Classical Treatment

In chapter 2 we derived an interpretation that the Josephson junction can be viewed as a single particle in certain potential field. Just like for a "real" particle, there's a certain limit after which the classical describtion of the Josephson junction is insufficient. The particle delocalizes and starts to go all the possible paths which lead to the same event, resulting in a wave behaviour. Beyond this limit we are led to use quantum mechanics to describe the state of the Josephson junction, as discussed first by Anderson [17] in 1964. But when will this behaviour become significant?

Let us analyze this problem for a current biased Josephson junction [32], the system discussed in section 2.6. In order to achieve quantum mechanical behaviour, we don't want that the Josephson junction is too much perturbed by its environment: incoherent processes with the surroundings lead to the

localization of the phase difference. We assume that the perturbation can be described by two sources: a thermal fluctuation and a damping of the environment. The first one is approximated by an average fluctuation of the energy k_BT. To avoid the incoherent mixing of the quantum states we demand that this is much lower than $\hbar\omega_p$, the energy difference of the states in the effective Josephson potential energy. Thus

$$\hbar\omega_p \gg k_BT. \tag{4.1}$$

For example if $T \sim 1\ K$, then we need $\omega_p \sim 10^{11}\ \frac{1}{s}$. We want also that the uncertainly in the energy, corresponding to a finite lifetime $\frac{C}{G}$ of the state, is much lower than the energy level separation. Therefore

$$\hbar\omega_p \gg \frac{C}{G}, \tag{4.2}$$

or equivalently $D \gg 1$ when using the definition (2.33). So we want an underdamped junction and a low temperature compared to the energy level separations of the states.

In practise, because the leads are attached to the junction, the shunting conductance will be determined by a parallel configuration of the quasiparticle and the high frequency lead resistance. The latter will be of an order 0.01 $\frac{1}{\Omega}$ and will usually determide the value for D. Also a "stray" conductance of the leads can be larger than a capasitance of a Josephson junction and has to be taken into account when determining the effective conductance of the system, but will be assumed to vanish in this situation. To fullfill all the demands, one needs a capasitance ~ 1 pF for a temperature 100 mK. This means that the dimensions of the junction are very small, of an order 1 μm.

The demands were achieved at the early 1980's [1, 2] and most of the first experiments studied MQT of the phase difference, which corresponds to the tunneling of φ across the tilted potential of the Josephson junction. The MQT was seen in various experiments [18, 19]. Afterwards there has been plenty of experimental verifications to the macroscopic quantum phenomenona. Observation of energy level quantization is a proof that the eigenstates of the Hamiltonian can be viewed as the basic states of the system. The ELQ has been observed using an rf-irradiation [20] and a method called rapid current ramping [21, 29]. A resonant tunneling between macroscopically distinct quantum states [22] has also been detected.

The recent study of small Josephson (or normal state) junctions has been focused on so-called single electronics, a study of charging effects caused by single electrons or Cooper pairs [42]. The charge variable Q is continuous even at the elementary scale because it describes the effective charge of Cooper pairs and ions placed nearby the electrodes. A change of this variable resulting from a tunneling is however discrete because only whole Cooper pairs can tunnel. If we want to see the effects resulting from the charging of

a single particles, the thermal or quantum fluctuations cannot average the charge variable. Therefore we can make analogous demands than (4.1) and (4.2) for the observation of the charging effects

$$E_c = \frac{e^2}{2C} \gg k_B T \tag{4.3}$$

$$G \ll \frac{e^2}{2\hbar} \approx \frac{1}{R_Q}. \tag{4.4}$$

If for example $T = 1\ K$, then equation (4.3) reads $C \ll 10^{-15}\ F$, which means that $A \leq (0.1\mu m)^2$, where A is the area of the junction. This shows that the behaviour is relevant only for mesoscopic Josephson junctions, which are usually called ultrasmall Josephson junctions.

Now we have problems: as discussed before, the effective conductance will become much larger than $\frac{1}{R_Q}$ and will lead to large fluctuations in the charge and no charging effects can be seen! Also the stray capasitance will mostly be much larger than the capasitance of an ultrasmall junction. These difficulties can be overcome by isolating the junction, extremely small high-impedance resistors must be inserted in the leads directly at the junction [24] or we have to study a system which contains many small junctions in series where the island left between the junctions is effectively isolated by the quasiparticle conductances of the nearby Josephson junctions. Especially if we now apply a voltage bias across the many Josephson junction system (actually mostly we have to assume a voltage bias because of the high stray capasitance), dynamics of the island can have quantum properties even if the collective state between the leads is assumed to be classical. A description for the special case of such a system is considered in more detailed in chapters 5 and 6.

4.2 Hamiltonian and its Eigenstates

Let us now consider how to write down the Hamiltonian of an isolated Josephson junction. Starting from the Lagrangian treatment we would obtain that φ and Q are conjugated variables. This is natural when thinking of the RCSJ-model, φ corresponds to a coordinate variable and Q to a momentum variable. One is led to the commutation relation

$$[\varphi, Q] = 2ei. \tag{4.5}$$

We see that the "delocalization constant" in this system is $2e$. The commutation relation implies that there is an uncertainly relation

$$\Delta\varphi \Delta Q = 2e, \tag{4.6}$$

which reflects the fact that for small Josephson junctions the state must be described by a wave function. For an isolated Josephson junction the operators can be presented in the φ-space

$$\hat{\varphi} = \varphi \tag{4.7}$$

$$\hat{Q} = -i2e\frac{\partial}{\partial\varphi}. \tag{4.8}$$

The Hamiltonian is the same as in equation (2.17) and we obtain

$$H = -4E_c\frac{\partial^2}{\partial\varphi^2} - E_j\cos(\varphi). \tag{4.9}$$

It turns out that the states must be distinguishable after a translation $\varphi \to \varphi + 2\pi$ [16]. Therefore, the corresponding Schrödinger equation is the same as for electrons in the ion lattice, well known from solid state physics. Eigenfunctions are Bloch wave functions and the corresponding eigenvalues are periodic functions of the quasimomentum k

$$\psi(\varphi)_k^n = u_k^n(\varphi)e^{ik} \tag{4.10}$$

$$u_k^n(\varphi + 2\pi) = u_k^n(\varphi) \tag{4.11}$$

$$E^n(k+1) = E^n(k). \tag{4.12}$$

In our case a more convenient variable is the quasicharge q (nothing to do with quasiparticles) defined as

$$q = 2ek. \tag{4.13}$$

It is interpreted as a charge which is given to the junction, for example by a current bias or some other doping mechanism. The junction can loose the charge Q by "collisions", which are described by the Josephson current in our case, but the value of q is changed only by an external doping.

4.3 Energy Bands

The shape and the energy of the eigenfunctions $\psi(\varphi)_q^n$ are crucially dependent on the relative magnitude of the charging and the coupling terms

$$s = \frac{E_j}{E_c}. \tag{4.14}$$

If $s \gg 1$, the Josephson potential energy dominates the Hamiltonian (4.9) and in the ground state $\psi(\varphi)_q^0$, φ is localised at the bottom of the Josephson potential. The interaction with the nearby cavities is vanishing and the system can be approximated locally by a harmonic oscillator. As a result, the energy of the state will have an exponentially small dependence on the

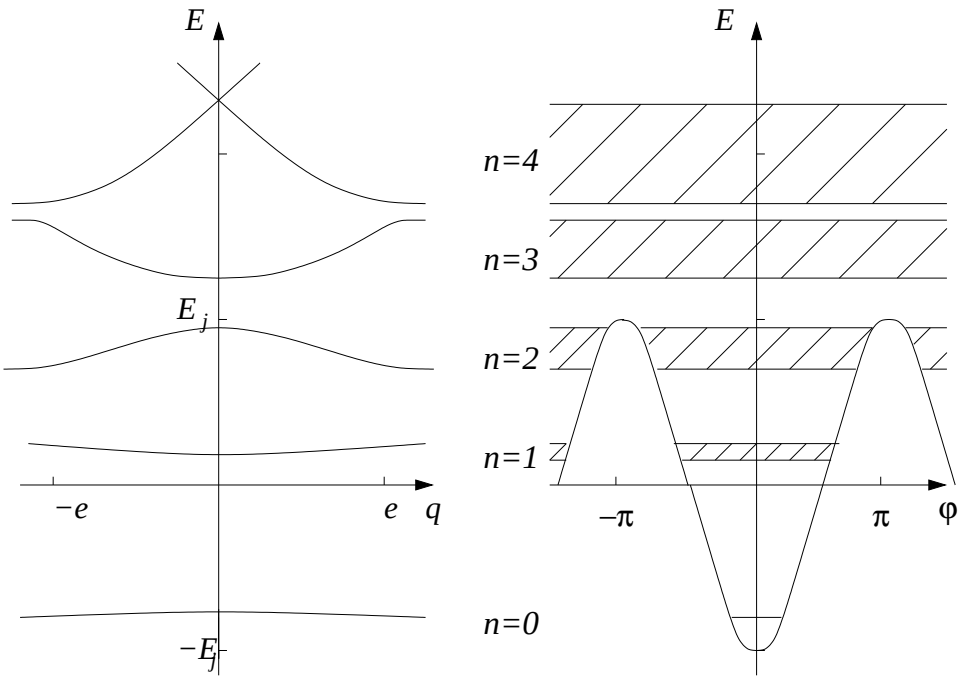

Figure 4.1: Energy bands and the Josephson potential energy when $s = 10$, the picture is taken from Ref. [16].

quasicharge. Energy bands are now energy levels, with the spacing of the harmonic oscillator's energy quantum $\hbar\omega_p$. However, high enough bands can interact with each other and delocalize. That introduces a periodic dependence of the quasicharge to the energy, as seen in figure 4.1.

If $s \ll 1$, the charging energy dominates the Hamiltonian and new behaviour is present. Now Q is localised and φ delocalized. The energy bands could be viewed to be formed from "local" parabolic momentum-energy curves placed on $Q = 0, 2e, 4e...$ These are then combined in a quantum mechanical superposition to form the energy band, as in figure 4.2. The energy of the band is $2e$ periodic and one period is called the Brillouin zone. Near the minimum of one parabolic curve, the fluctuation of the charge is very small and only some constant differs the quasicharge and the real charge of the electrodes

$$Q = q + 2en, \tag{4.15}$$

where n is an integer. In the vicinity of the points $e + 2em$, where m is an integer, the state is a superposition of two charge states coming from different parabolic centers and equation (4.15) is not valid.

One should note also that we cannot anymore think of a "classical voltage" $\frac{Q}{C}$ across the junction at some given time, the charge can be highly delocalized and so is the voltage also. Of course we cannot do this ideally

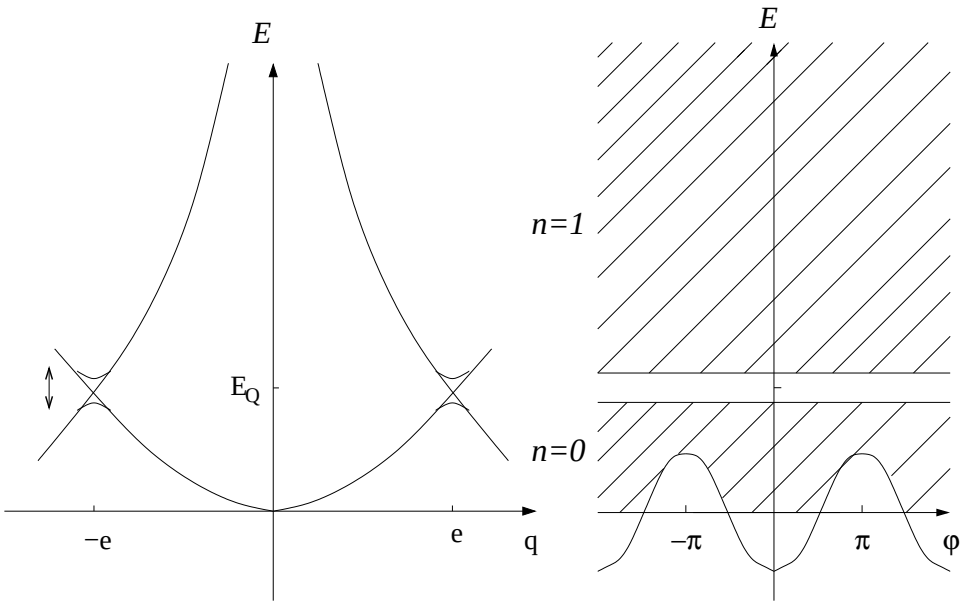

Figure 4.2: Energy bands and the Josephson potential energy when $s = \frac{2}{5}$, the picture is taken from Ref. [16].

in the classical limit either, but there the charge of a single electron doesn't mean anything (typical capasitances $C \geq 10^{-10}F$) and a wave packet can be easily constructed with a vanishing relative error on the voltage. In all the limits there is however a well defined mean voltage V (quantum average) across the junction which can be a function of time, if the state is for some reason changing.

4.4 Discreteness of the Charge

We have solved the Schrödinger equation for an isolated Josephson junction in φ space by using "continuous" operator $-i2e\frac{\partial}{\partial\varphi}$ for the charge of the electrodes. Especially in the limit $s \ll 1$ one can consider the justification for the procedure because in elementary processes of the Josephson tunneling, the charge isn't a continuous parameter, unlike the momentum of a real particle. Also when we will describe the two Josephson junction system in series, the charge variable can have only discrete values. Does the continuous solution describe also the discrete system?

One can get rid of this "problem" by using the BCS theory. When the superconductors are far away, the particle exchange between them is not possible. When they are brought close together, the tunneling can occur with the help of the Josephson potential energy. Assuming that there were originally M Cooper pairs in the left conductor and N cooper pairs in the

right one, we can describe the state of an isolated junction with the help of two basic set of states, the phase difference eigenstates $|\psi_\varphi\rangle$ and the particle (Cooper pair) exchange eigenstates $|\psi_j\rangle$ [30]. These could be viewed to be a subspace from the particle number and the phase eigenstates of the two superconductors. In the state $|\psi_\varphi\rangle$ the macroscopic phase difference between between the superconductors is determined but the particle exhange number is undetermined. This describes the classical state of the Josephson junction. The state $|\psi_j\rangle$ corresponds to the determined number of exchanged Cooper pairs and undetermined phase difference. The uncertainly of the states reflects the relation (4.6).

Eigenstates of the Hamiltonian can be written as a superposition of the particle exchange eiqenstates

$$|a\rangle = \sum_j a_j |j\rangle, \tag{4.16}$$

where j is an integer and denotes for how many Cooper pairs are exchanged. In the same basis, the Hamiltonian can be written in a form

$$\sum_j (2j - Q_0/e)^2 E_c |j\rangle\langle j| - \frac{E_j}{2}(|j+1\rangle\langle j| + |j-1\rangle\langle j|), \tag{4.17}$$

where Q_0 is a charge injected from outside to the electrodes. The first term in (4.17) describes the Coulomb interaction between the electrodes and the second term is the Josephson potential energy $-E_j \cos(\varphi)$. The latter can be deduced by writing

$$-E_j \cos(\varphi) = -\frac{E_j}{2}\left(e^{i\varphi} + e^{-i\varphi}\right). \tag{4.18}$$

In quantum mechanics $e^{i\hat{\varphi}}$ is a momentum shift operator, which increases the momentum by one "quantum constant", which in our case is simply $2e$. We see that the Josephson potential energy in (4.17) takes care of the tunneling to both directions across the insulating barrier. We assume now that solving the Hamiltonian (4.9) is equivalent to solving equation (4.17) with $q = Q_0 + n2e$, where n is some integer.

Assuming that $E_c = 0$ we obtain that the eigenstates are just the phase difference eigenstates with the eigenvalues $-E_j \cos(\varphi)$, no kinetics are present. When $s \gg 1$ but $E_c \neq 0$ the solution is a superposition of the phase difference states. The amplitudes can be obtained from harmonic oscillator's eigenfunctions, which are Gaussian and independent of q, as discussed before. In the limit $s \ll 1$ the eigenstates are close to the charge eigenstates and the quasicharge has a crucial contribution. Now if we are in the local bottom of the parabolic potential (for example $q = 0$), the ground state eigenfunction is approximately [16]

$$\psi(\varphi)_0^0 = 1 + \frac{s}{4}\left(e^{i\varphi} + e^{-i\varphi}\right) = 1 + \frac{s}{2}\cos(\varphi). \tag{4.19}$$

Using the relation (4.18) we deduce the corresponding BCS solution

$$|\psi\rangle_0^0 = |0\rangle + \frac{s}{4}(|1\rangle + |-1\rangle). \tag{4.20}$$

This gives a physical insight to the solution. Because $s \ll 1$, the (virtual) Cooper pair exchange between the electrodes is almost vanishing and the system is in the state where practically no particles are exhanged. If we are in the region $q = e$, the solution is almost degenerated as seen from figure 4.2. The Bloch wave functions for the ground state and the first excited state can be approximated by [16]

$$\psi(\varphi)_e^0 = \frac{1}{\sqrt{2}}\left(e^{\frac{i\varphi}{2}} + e^{\frac{-i\varphi}{2}}\right) \tag{4.21}$$

$$\psi(\varphi)_e^1 = \frac{1}{\sqrt{2}}\left(e^{\frac{i\varphi}{2}} - e^{\frac{-i\varphi}{2}}\right). \tag{4.22}$$

The corresponding solutions in the BCS theory are

$$|\psi^0\rangle_e^0 = \frac{1}{\sqrt{2}}(|0\rangle + |1\rangle) \tag{4.23}$$

$$|\psi^1\rangle_e^1 = \frac{1}{\sqrt{2}}(|0\rangle - |1\rangle). \tag{4.24}$$

We see that in each of the two solutions there is a linear combination of two charge states. This explains why the quasicharge and the true charge Q are not equivalent in this region. The antisymmetric combination of the states is more energetic and the symmetric is the ground state. The energy E_j differs the two solutions.

The charge state in the limit $q = e$ is a possible candidate for the realisation of a quantum logic state, the qubit [27]. For possible applications in the quantum computing or in the nanotechnology Josephson junctions are nice devices since they are easily coupled to the electrical circuit and that way to other devices also. However, true realisations in these fields are far from today.

4.5 Bloch Oscillations in Small Josephson Junctions

The Bloch oscillation is a phenomenon well known from the theory of electrons in solid [23] and it basicly reflects the quasicharge dependence of the Bloch wave functions. The Bloch oscillations have been very hard to observe in metals but fortunately the same phenomenon can occur in other kind of systems also. One of these is a current biased small Josephson junction where observations of the Bloch oscillations have been made [24]. The identification can be made by applying a small ac-current component to the

dc-biased Josephson junction which will phase-lock the oscillations, resulting steps in the $I-V$ curve. This is a quantum analog effect of the Shapiro steps. Possible applications of the Bloch oscillations in the nanotechnology have been also proposed [25].

Let us discuss shortly how the Bloch oscillations could occur. Suppose that there is a weak current bias to the system discussed in section 4.2. We will also take into account a small quasiparticle conductance G. From the tilted Josephson potential energy (2.32) we know how the drive current affects the Hamiltonian, thus [16]

$$H = \frac{Q^2}{2C} - E_j \cos(\varphi) - \frac{\hbar}{2e} I(t)\varphi + \frac{\hbar}{2e} I_q(x)\varphi + H_q(x), \tag{4.25}$$

where $\frac{\hbar}{2e} I(t)$ describes the drive current, $\frac{\hbar}{2e} I_q(x)$ the quasiparticle current and $H_q(x)$ is the Hamiltonian of the quasiparticle space. The coordinate x symbolizes the fact that the quasiparticle current can't be described in the φ-space, it has its own coordinate representation. However, it changes Q so the two subspaces have a coupling, which is described by the term $\frac{\hbar}{2e} I_q(t)\varphi$.

Using the assumption of a weak current bias and a low quasiparticle conductance, we can obtain the solution by using the perturbation theory when taking the Bloch eigenstates as the unperturbed states. Let us assume that $k_B T \ll \Delta^0$ where Δ^0 is the (lowest) energy difference between the ground state and the first excited state. Then the effect of the perturbation can be written in a very simple Langevin-type equation for the quasicharge operator in the Heisenberg picture

$$\dot{q} = I(t) - G\frac{dE_q^0}{dq} - \tilde{I}(t), \tag{4.26}$$

where $\tilde{I}(t)$ describes fluctuations of the current.

Let us assume that $\tilde{I}(t) = 0$, which can be made if the quasiparticle conductance and the temperature are low enough [16]. We can now interpret that q is a semiclassical variable and $\frac{dE_q^0}{dq}$ is the voltage across the junction (at least a quantum average of it). If $I(t)$ is low, the system can have a stable solution when the quasiparticle current and the drive current cancel each other ($I(t) = GV(t)$). The quasicharge, the voltage and the current are now constants, no Josephson supercurrent is present because its quantum average vanishes. If $I(t)$ is high enough, the quasicharge will have a permanent motion in the energy band and the energy of the state will be a periodic function of time with an angular frequency ω_B. Time averaging the components in equation (4.26) we obtain the Bloch frequency

$$\omega_B = \frac{\pi}{e}(I - GV). \tag{4.27}$$

The voltage and the quasicharge are oscillating with the frequency (4.27) and there's a nonvanishing net current through the junction. The phenomenon

is called the Bloch oscillation. Physically one oscillation corresponds to a tunneling of one Cooper pair.

The tunneling process can be viewed in detail when using the BCS solution. Let us assume that $s \ll 1$ so the energy is highly dependent on the quasicharge. When $q \approx 0$ equation (4.15) is valid and equation (4.26) can be written in the form

$$\dot{Q} = I(t) - GV(t). \tag{4.28}$$

At this stage the drive current is recharging the capasitor. When the system arrives in the reqion $q \approx e$, there's an intense reflection of the Bloch waves from the top of the Josephson potential and the quantum average of the Josephson supercurrent won't vanish. In the BCS solution this means that the system starts to move from one charge state to another, single Cooper pair tunnels across the junction. After this stage, the drive current starts to reload the capasitor again for another tunneling event to happen at $q \approx 3e$.

In the case $s \gg 1$ situation is more complicated. The quasicharge dependence of the energy is small but not vansihing. The wave function is localized in one of the wells so the charge is highly delocalized, the state is a superposition of many different charge states. However, the process must be analogous to the previous one, when the quasicharge has moved from the region $q = 0$ to $q = 2e$ the state has moved from one brillioun zone to another. This means that there has had to be effectively one Cooper pair transfer across the junction to the current source between the states $q = 0$ and $q = 2e$.

In simple terms, the Bloch oscillation in a current biased Josephson junction is a periodic and discrete Cooper pair transfer over the insulating barrier joined with a charge transfer from the capasitor to the current source. This is an example of a phenomenon which deals with a single charging of Cooper pairs.

4.6 Effect of the charging to Josephson Coupling Energy

In chapter 2 we discussed that the critical current of a Josephson junction can be written in the form (2.9). We can calculate I_c by measuring the normal state resistance and the BCS gap function of the system and then compare this to the experimental results of I_c. The agreement with large junctions is exellent but for mesoscopic junctions disagreement is found [14, 31, 40] and many possible explanations for the effect is given [26]. For example, it has been proposed that this phenomenon arises because of the charging effects present in the junction and a formula for the new critical

current I_c' is given [28]

$$I_c' = \frac{I_c}{\pi^2}\sqrt{\frac{2E_j}{E_c}}. \tag{4.29}$$

However, even this isn't consistent with the experimental results and there are still open questions. Generally the exact value of E_j has to be fitted using the experimental data. This lowers the "purity" of the theoretical part.

Chapter 5

Inelastic Cooper Pair Tunneling

In this chapter we will concentrate on describing a voltage biased small Josephson junction by using so-called $P(E)$-theory. We want to calculate the $I-V$ curve resulting from excitations and dissipations of macroscopic quantum states present in the circuit. In the $P(E)$-theory a dissipative environment of the Josephson junction can be described in a relatively simple form and the current-voltage characteristics are easy to evaluate. As a result we will see that a small Josephson junction with $s \ll 1$ could be used as a probe for the macroscopic quantum phenomena. At first we will discuss the time dependence of a voltage biased many Josephson junction system when no dissipative tunneling processes are present. Then we show how these can be included using the $P(E)$-theory. After that we discuss the properties and interpretation of the $P(E)$-function and important cases of low and high impedance environments. Finally we will solve the $P(E)$-function for an inductive environment. This chapter is mostly based on the discussions made by Ingold & Nazarov [33] and Ingold & Grabert [36].

5.1 Exact Nondissipative Solution

In the current biased Josephson junction case the leads had an huge impact to the system, actually the ultrasmall junctions ($C \leq 10^{-15}\ F$) are now overdamped! The easiest way to circuimwent this problem is to use two Josephson junctions in series. Because of the high stray capasitances of the leads, this system is usually effectively voltage biased. As a result, one can assume that the phase difference accross the system is a classical variable and the phase related to the island between the conductors can have quantum fluctuations.

We want to solve the time evolution of this system and then calculate the current as a function of the voltage. For two Josephson junctions in

series one is forced to describe the system in the interaction picture (or using some other time dependent method), because the Hamiltonian becomes time dependent (effect of the voltage bias). In the same fashion as in chapter 2, we would finally obtain an oscillative quantum mechanical system. Then we could take the quantum average of the Josephson supercurrent operator $I_c \sin(\varphi_i)$ and obtain the current. As a result, the net current vanishes for all voltages $V \neq 0$. Why? Because there is no dissipation mechanism present. If there's a current over some constant voltage difference, energy is released to the system. If no dissipation is present, the energy increases until the current must turn back to conserve the energy. In order to calculate a nonvanishing value for the net current, we need to include dissipative current processes. Because all the Cooper pairs are in the same state and they won't give any rise to the dissipation, this leads to the idea of an energy exchange between the junction and its electromagnetic environment.

5.2 Electromagnetic Environment

In this section we will construct a dissipative electromagnetic environment which describes the space (and therefore also the coupling) between a voltage source and a probe junction. This space contains all the possible components near the probe junction and the leads to the voltage source. The environment and the applied voltage will then determine the dynamics of the system when time goes on. This will include energy exchange between the tunneling Cooper pair and the environment and finally dissipation of this energy. Classically the dynamics can be calculated by using an impedance of the environment and the same thing is the aim in the $P(E)$-theory. Using the same kind of model, MQT of the phase difference (partly discussed in section 4.1) was studied under dissipative processes leading to a damping [1, 38]. However, we are now dealing with a voltage bias and that model won't be valid for this case.

Before writing down the Hamiltonian of the environment, we will study a voltage biased LC-circuit which will be the basic building block for the environment. We won't take the Josephson potential energy in account yet, but we assume that φ across the junction is well defined. We also assume that the phase difference between the leads is a classical variable but the phase difference across the junction can have quantum fluctuations. We obtain for the Lagrangian

$$\mathcal{L} = \frac{C}{2}\left(\frac{\hbar}{2e}\dot{\varphi}\right)^2 - \frac{1}{2L}\left(\frac{\hbar}{2e}\right)^2\left(\varphi - \frac{2e}{\hbar}Vt\right)^2. \tag{5.1}$$

The first term in (5.1) is the familiar charging energy of the capasitor and the second is the (magnetic field) energy of an inductor which can be written with the help of the phase difference across the inductor ($\frac{2e}{\hbar}Vt - \varphi$). From

(5.1) we deduce that the mean value of φ starts to move with a velocity $\frac{2e}{\hbar}V$, implying that there's a mean voltage V across the junction. We do a change of variables to eliminate the time dependence and obtain the Hamiltonian as a function of fluctuations around the mean values. We could view that we are going to the local coordinate reference of a moving harmonic potential. We insert

$$\varphi = \tilde{\varphi} + \frac{2e}{\hbar}Vt, \tag{5.2}$$

and obtain

$$\mathcal{L} = \frac{C}{2}\left(\frac{\hbar}{2e}\dot{\tilde{\varphi}} + V\right)^2 - \frac{1}{2L}\left(\frac{\hbar}{2e}\right)^2\tilde{\varphi}^2. \tag{5.3}$$

Turning now to the Hamiltonian formalism, we obtain (by neglegting the irrelevant constants)

$$H = \frac{1}{2C}\tilde{Q}^2 + \frac{1}{2L}\left(\frac{\hbar}{2e}\right)^2\tilde{\varphi}^2, \tag{5.4}$$

where

$$\tilde{Q} = Q - CV, \tag{5.5}$$

is the fluctuation of the charge around the mean charge and $Q = C\frac{\hbar}{2e}\dot{\varphi}$. The fluctuations can be now viewed as conjugated variables in the Hamiltonian formalism (to be precise we do a canonical transformation of the momentum to enter the fluctuation basis because in equation (5.3) Q is the conjugated variable of $\tilde{\varphi}$). The commutator between the new variables is as before

$$[\tilde{\varphi}, \tilde{Q}] = 2ei. \tag{5.6}$$

The Hamiltonian (5.4) demonstrates the equivalence between an LC-circuit and a harmonic oscillator. The harmonic behaviour is now obtained for the fluctuations around the mean values.

To describe the dissipation, we phenomenologically introduce a Hamiltonian which couples the fluctuations to infinite many LC circuits

$$H_{\text{env}} = \frac{\tilde{Q}^2}{2C} + \sum_{n=1}^{\infty}\left[\frac{q_n^2}{2C_n} + \left(\frac{\hbar}{2e}\right)^2\frac{1}{2L_n}(\tilde{\varphi} - \varphi_n)^2\right]. \tag{5.7}$$

The voltage source is taken into account in the definitions of $\tilde{Q}$ and $\tilde{\varphi}$ as shown before. q_n can be viewed as the charge operator of the n:th oscillator and so on. Using the Heisenberg equations of motion for the operators $\tilde{Q}$, $\tilde{\varphi}$, q_n and φ_n we can show that this Hamiltonian effectively describes the classical relaxation of the charge. The relaxation can be described using the

"classical" impedance $Z(\omega)$ of the environment, which can be calculated in the form

$$Z(\omega) = \left(\int_0^\infty e^{-i\omega t} \sum_{n=1}^{\infty} \frac{1}{L_n} \cos(\omega_n t) dt \right)^{-1}, \tag{5.8}$$

where ω_n is the plasma frequency of the n:th environmental LC circuit. This is a Fourier transform of an arbitrary cosine series which indicates that any impedance can be achieved.

The Hamiltonian (5.7) is now on used as an environmental part of the total Hamiltonian when deriving the results for the current voltage characteristics of the system. At the end, we don't need to use this complex Hamiltonian, all we need to know is the impedance of the environment which can be evaluated quite easily for the most of the situations.

5.3 Tunneling Hamiltonian

We will now write the total Hamiltonian of the system shown in figure 5.1. When no quasiparticles are present, it is just the sum of the environmental

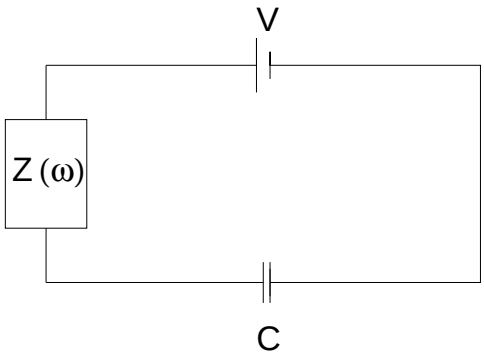

Figure 5.1: Environmental impedance Z in series with capasitor.

part and the Josephson potential energy. So we have

$$H = H_{\text{env}} - E_j \cos(\varphi). \tag{5.9}$$

We rewrite the Josephson term as done in equation (4.18) and identify the Cooper pair transfer operators in the two directions. Our aim is to use $E_j \cos(\varphi)$ as a small perturbation which affects tunneling across the junction and calculate the current by using the golden rule approximation for the transition rates. This means that we have to assume a small E_j and a fast dissipation to the ground state between the transitions. The environmental Hamiltonian therefore takes the control of the unperturbed state and the mean voltage across the junction is V. As described before, the Hamiltonian couples to the fluctuations around the mean values and therefore the

perturbation is written in an analogous form than in equation (5.2). Using the transition rate calculus for a harmonic perturbation ($e^{\pm i\omega t}$ dependence) we obtain

$$\Gamma^{\pm}(V) = \frac{\pi}{2\hbar}E_j^2 \sum_{R,R'} |\langle R'|e^{\mp i\tilde{\varphi}}|R\rangle|^2 P_\beta(R)\delta(E_R - E_{R'} \pm 2eV). \tag{5.10}$$

Here $|R\rangle$ and $|R'\rangle$ are eigenstates of the environmental Hamiltonian and P_β is the thermal propability distribution for the unperturbed state. As we see, the δ-function takes care of the energy conservation. The harmonic perturbation induces an energy absorbation or emission (just like in the case of the stimulated emission) and it introduces a term $\frac{2eV}{\hbar}\hbar = 2eV$ into the δ-function. This can be interpreted that because there's a voltage across the junction, the energy change in the Cooper pair transition across the junction is $2eV$ and it must be absorbed or emitted by the environment, depending on the tunneling direction.

We want to eliminate the explicit dependence of the environmental states and describe them only by using a classical impedance of the system. The first step in this direction can be made by transforming the δ-function to the integral form

$$\delta(E_R - E_{R'} + 2eV) = \frac{1}{2\pi\hbar}\int_{-\infty}^{\infty} \exp\left(\frac{i}{\hbar}(E_R - E_{R'} + 2eV)t\right) dt. \tag{5.11}$$

Now we can write the part of (5.10) containing the environmental dependence in the form

$$\begin{aligned} & e^{\frac{i}{\hbar}(E_R - E_{R'})t}|\langle R'|e^{\mp i\tilde{\varphi}}|R\rangle|^2 = e^{\frac{i}{\hbar}(E_R - E_{R'})t}\langle R|e^{\pm i\tilde{\varphi}}|R'\rangle\langle R'|e^{\mp i\tilde{\varphi}}|R\rangle \\ =&\langle R|e^{\frac{i}{\hbar}H_{\rm env}t}e^{\pm i\tilde{\varphi}}e^{-\frac{i}{\hbar}H_{\rm env}t}|R'\rangle\langle R'|e^{\mp i\tilde{\varphi}}|R\rangle \\ =&\langle R|e^{\pm i\tilde{\varphi}(t)}|R'\rangle\langle R'|e^{\mp i\tilde{\varphi}(0)}|R\rangle, \end{aligned} \tag{5.12}$$

where

$$e^{\tilde{\varphi}(t)} = e^{\frac{i}{\hbar}H_{\rm env}t}e^{i\tilde{\varphi}}e^{-\frac{i}{\hbar}H_{\rm env}t}, \tag{5.13}$$

is the operator $e^{\tilde{\varphi}}$ in the Heisenberg picture. Using equations (5.11) and (5.12) one can trace out the environmental freedoms in equation (5.10) and obtain

$$\Gamma^{\pm}(V) = \frac{E_j^2}{4\hbar^2}\int_{-\infty}^{\infty} \exp\left(\pm\frac{i}{\hbar}2eVt\right)\langle e^{\pm i\tilde{\varphi}(t)}e^{\mp i\tilde{\varphi}(0)}\rangle dt, \tag{5.14}$$

where $\langle A\rangle$ means an equilibrium correlation function of the operator A. Using the generalized Wick theorem we can define the phase-phase correlation function $J(t)$

$$\langle e^{\pm i\tilde{\varphi}(t)}e^{\mp i\tilde{\varphi}(0)}\rangle = e^{\langle[\tilde{\varphi}(t)-\tilde{\varphi}(0)]\tilde{\varphi}(0)\rangle} = e^{J(t)} \tag{5.15}$$

$$J(t) = \langle[\tilde{\varphi}(t) - \tilde{\varphi}(0)]\tilde{\varphi}(0)\rangle. \tag{5.16}$$

The $P(E)$-function is defined as a Fourier transform of the correlation function

$$P(E) = \frac{1}{2\pi\hbar}\int_{-\infty}^{\infty} \exp\left[J(t) + \frac{i}{\hbar}Et\right] dt. \tag{5.17}$$

It is interpreted as a probability to emit energy E from the probe junction to the environment. Using (5.14-17) we obtain

$$\Gamma^{\pm}(V) = \frac{\pi}{2\hbar}E_j^2 P(\pm 2eV). \tag{5.18}$$

We can now write the total current across the junction with the help of the transition rates. One transition corresponds to the tunneling of one Cooper pair, so we have

$$I = 2e(\Gamma^+ - \Gamma^-) = \frac{e\pi}{\hbar}E_j^2[P(2eV) - P(-2eV)]. \tag{5.19}$$

What is left is to obtain the dependence between $P(E)$ and $Z(\omega)$. The effect of the environmental degrees of freedom on the charge and the phase degrees of freedom is twofold. Firstly, they produce a damping term which relaxes the charge to the equilibrium after a tunneling event. This effect can be described by a classical impedance $Z(\omega)$ due to Ehrenfest theorem. Secondly, the quantum fluctuations in the environment will have an effect to the correlation functions, for example the one in (5.16). Since the damping and fluctuations have the same microscopic origin, they are not independent and are related by so-called fluctuation-dissipation theorem. With the help of that we would finally obtain

$$J(t) = 2\int_0^{\infty} \frac{d\omega}{\omega}\frac{\mathrm{Re}Z_t(\omega)}{R_Q}\left[\coth\left(\frac{1}{2}\beta\hbar\omega\right)(\cos(\omega t) - 1) - i\sin(\omega t)\right], \tag{5.20}$$

where $Z_t(\omega)$ is the tunneling impedance, an effective impedance of the circuit as seen from the junction. It consist of a parallel contributions of the capasitance C (described by an impedance $\frac{1}{iC\omega}$) and the impedance $Z(\omega)$

$$Z_t^{-1}(\omega) = \frac{1}{i\omega C + Z^{-1}(\omega)}. \tag{5.21}$$

For any external impedance, we can calculate the $P(E)$-function by integrating equations (5.17) and (5.20). Then we can obtain the current as a function of the voltage using (5.19).

5.4 General Properties of $P(E)$

We interpreted $P(E)$ to be the probability to emit an energy E to the external circuit. Correspondingly, $P(-E)$ is the probability for an absorbtion

of an energy E. If for example $T = 0$, then $P(-E) = 0$ for all $E > 0$ and therefore $P(E)$ is proportional to the current. This is natural because in the superconducting state, there are no "electronic" degrees of freedom for Cooper pairs as there is for quasiparticles. Cooper pairs have only one state to "land" on the other side of the junction and the energy released has to be absorbed elsewhere, it excites a reservoir state. As a result, $P(2eV)$ is proportional to I which is the most important feature of the $P(E)$-function in the superconducting case. Measuring the $I - V$ curve at $T \approx 0$ we are actually measuring $P(E)$ and therefore also the energy level structure of the electromagnetic environment. This is the reason why we call this small Josephson junction as the probe junction.

Using equation (5.16) we obtain for the general temperature case the first sum rule

$$\int_{-\infty}^{\infty} P(E)dE = e^{J(0)} = 1. \tag{5.22}$$

This confirms our interpretation of $P(E)$ as a probability. The second sum rule is obtained by a partial integration

$$\int_{-\infty}^{\infty} EP(E)dE = i\hbar J'(0) = 4E_c, \tag{5.23}$$

which means that the mean value of E is $4E_c$, the charging energy of one Cooper pair. The thermal dependence of the backward tunneling can be derived in the form

$$P(-E) = e^{-\beta E}P(E), \tag{5.24}$$

which reflects the thermal distribution $P_\beta(R)$ of the initial states.

5.5 High and Low Impedance Environments

We will now solve the $P(E)$-function for two simply, but very important cases: high and low impedance environments. The low impedance environment is defined as $Z(\omega) = 0$. This is practically achieved if $Z(\omega) = R \ll R_Q$. The phase fluctuations described by equation (5.20) almost vanish and we can approximate

$$P(E) = \delta(E). \tag{5.25}$$

This corresponds to the fact that in the absence of environmental modes (which could absorb energy), only elastic tunneling is possible. The voltage source transfers the tunneled Cooper pair almost immediately through the circuit and the system acts as it would be connected only to an ideal voltage source. This is called the global rule of tunneling: the circuit acts as an

entity and all the energy prosesses needed happen in the voltage source, no local energy transfers are present. The $P(E)$-function (5.25) violates equation (5.23) because the impedance is assumed to be zero. For a small impedance the rule becomes valid but still the $P(E)$-function is close to the δ-function.

The opposite limit to the previous case is the high impedance environment. It is defined as an impedance which is much larger than R_Q. This could be achieved when $Z(\omega) = R$, $R \gg R_Q$, i.e. the external impedance is formed from a "large" ohmic resistor. We obtain for the tunneling impedance (5.21)

$$Z_t(\omega) = \frac{R}{1 + i\omega RC}. \tag{5.26}$$

The real part of this aproaches to $\frac{\pi}{C}\delta(\omega)$ when $R \to \infty$. It can be shown that for very low temperatures $P(E)$ can be approximated by

$$P(E) = \delta(E - 4E_c). \tag{5.27}$$

This implies that the tunneling is possible only when $2eV = 4E_c$. It can be understood qualitatively when considering the junction region only locally. The voltage source cannot balance the electrodes immediately after the tunneling because the resistor inhibits a fast recharging. As a result, the Coulomb energy of the electrodes changes

$$\Delta E_c = \frac{Q^2}{2C} - \frac{(Q - 2e)^2}{2C}. \tag{5.28}$$

Practically the interaction to the outer world vanishes and the resistor won't generate any "quantum states" which could help the tunneling (equivalent to that there are no resonances at Z_t expect at in $\omega = 0$). Therefore this energy change has to vanish. That is equivalent to that $2eV = 4E_c$. Afterwards, the voltage source recharges the capasitor and the system is finally at the same state than before the tunneling. This is called the local rule of tunneling since the relevant events occur only locally.

The fact that tunneling cannot occur below $V = \frac{2E_c}{e}$ is a result from that the Coulomb interaction would increase the energy of the state. The phenomenon is called the Coulomb blockade of tunneling. There are many phenomena under this name, but they all have a common feature: the tunneling of a single charge is forbidden (or highly suppressed) because it increases the energy. One could view that when $s \ll 1$ the ground state of an isolated Josephson junction is suffering from the Coulomb blockade, a quantum fluctuation even of a single Cooper pair is very unlikely because it is energetically unfavorable. The Coulomb blockade of tunneling has been detected experimentally in various experiments [34, 35] and it is clear that the possibility of the controlling of a single charge might have important applications in the future.

A phenomenon close to the Coulomb blockade is a Coulomb gap which is present in the normal state behaviour. The tunneling in these junctions is possible for all voltages after the region $2eV = E_c$ because of electronic degrees of freedom. However, the normal state resistance is "shifted" by an amount of $\frac{e}{2C}$ resulting in a shift in an ohmic $I-V$-curve. This phenomenon can be used to measure the capasitance of the junction.

5.6 Inductive Environment

Let us consider a situation when the external circuit consist only from an ideal inductor. In this case we could take the environment (5.7) rather literally. We start by writing down the tunneling impedance of the circuit. The inductor is described by an impedance $i\omega L$ so we have

$$Z_t(\omega) = \frac{1}{C}\frac{i\omega}{\omega_p^2 - (\omega - i\epsilon)^2}, \tag{5.29}$$

where ω_p is the plasma frequency of the corresponding LC-oscillator. A small complex variable $i\epsilon$ is added to ω to get the correct result for the real part, for which we obtain (in the limit $\epsilon \to 0$)

$$\mathrm{Re}Z_t(\omega) = \frac{\pi}{2C}[\delta(\omega - \omega_p) + \delta(\omega + \omega_p)]. \tag{5.30}$$

There are clear quantum mechanical resonances present in the environment, arising from the LC-oscillations. Using equations (5.17), (5.20) and (5.30) we can obtain

$$\begin{aligned} P(E) &= \frac{1}{2\pi\hbar}\int_{-\infty}^{\infty} dt \\ &\exp\left[\rho\left(\coth(\frac{\beta\hbar\omega_p}{2})(\cos(\omega_p t) - 1) - i\sin(\omega_p t)\right) + \frac{i}{\hbar}Et\right], \end{aligned} \tag{5.31}$$

where

$$\rho = \frac{4E_c}{\hbar\omega_p}, \tag{5.32}$$

compares the charging energy and the plasma frequency of the environment. We are interested in the situation when $T = 0$ because then its simple physical origin becomes apparent, no thermal activitations are present. Then the solution of (5.31) can be expressed analytically

$$P(E) = \sum_{k=0}^{\infty} \rho_k \delta(E - k\hbar\omega_p), \tag{5.33}$$

where

$$\rho_k = e^{-\rho}\frac{\rho^k}{k!}, \tag{5.34}$$

is the probability to emit k oscillator quanta. We see that ρ_k obeys the Poissonian distribution, therefore quanta are emitted independently. The interpretation is as follows. The environment is analogous to a harmonic oscillator and its energy levels are therefore spaced by $\hbar\omega_p$. The probabilities for the excitations to the higher levels under the perturbation are obtained from equation (5.34). The effect of the temperature is to form a distribution of the initial states from where the system absorbs or emits quanta. This effect is however vanishingly small if $\hbar\omega_p \gg k_B T$.

We can generalize the result (5.33) for two or even more environmental modes present in the system at $T \approx 0$ (assuming a Poissonian distribution for them). If our system has effectively two independent LC oscillators in series, i.e. the tunneling impedance shows resonances at two different places for $\omega > 0$, the $P(E)$-function can be deduced by multiplying the probabilities of the two independent events

$$P(E) = e^{-\rho_a-\rho_b}\sum_{n=0,m=0}^{\infty}\frac{\rho_a^n\rho_b^m}{n!m!}\delta(E - n\hbar\omega_a - m\hbar\omega_b). \tag{5.35}$$

We see that not only there are transitions from the individual cases, but also multiphoton transitions where n quanta are absorbed to the oscillator a and m quanta to the oscillator b. The $P(E)$-function shows resonance whenever the energy E can be expressed as a sum $n\hbar\omega_a + m\hbar\omega_b$, and the corresponding probability is the product of the two probabilities. One should however note that, for example, the case of two inductors in the environment doensn't give rise to a tunneling impedance with two modes, it needs a more complex system.

When also a resistance is included, one is forced to use numerical methods when calculating the $P(E)$-function. The integrals (5.17) and (5.20) converge slowly but for finite temperatures one can calculate the $P(E)$-function easier with the help of the integral equation found in Ref. [38]. The effect of a small resistance in series with an inductor is approximately to broaden δ-functions to Lorenzian peaks and make the current finite. To describe this effect, we define the quality factor Q

$$Q = \frac{1}{RC\omega_p}. \tag{5.36}$$

We see that the quality factor is the inverse of D defined in equation (2.33) in the context of a current biased Josephson junction, $Q = \frac{1}{D}$. This is because of the difference in the drive sources. When having a voltage source we want a fast recharging to the equilibrium to have clear "voltage states",

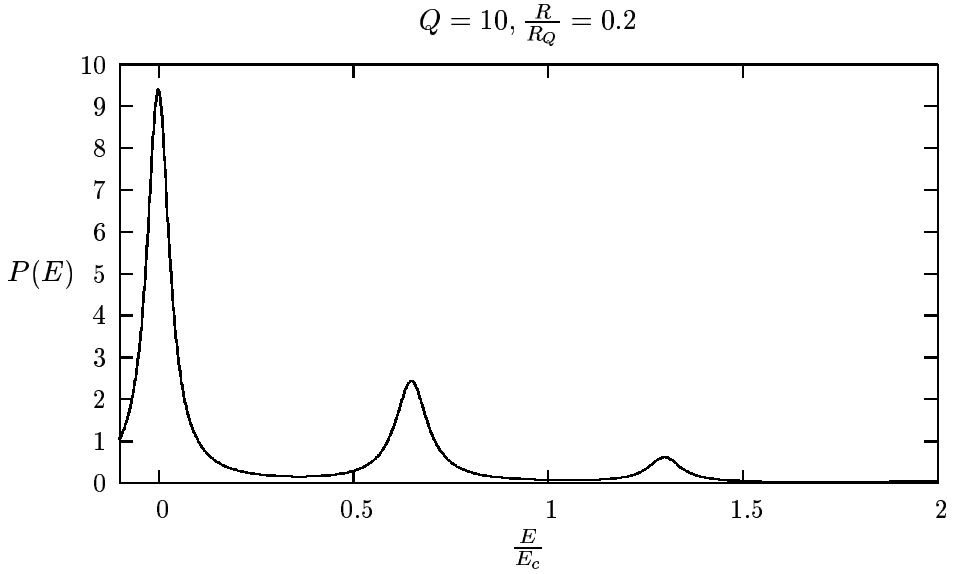

Figure 5.2: The P(E)-function calculated in Ref. [40] using the integral equation taken from Ref. [38].

the resistor is analyzed in a series connection and therefore it has to be small. When having a current source we want as slow relaxation as possible to have no quantum fluctuation of the energy, the resistor is analyzed in a parallel connection and therefore it has to be as high as possible. We see now that the high frequency impedance (which was a big problem in the current biased model) won't usually give arise any difficulties in this case. Example of a $P(E)$-function when $Q \gg 1$ is shown in figure 5.2.

An impressive indication of the inelastic tunneling was made by Holst [37] in a situation where two load resistors were used to form a tranmission line resonator environment for the probe junction. In this situation a tunneling impedance of the leads shows clear resonances at certain frequencies. These were then seen in the experinment as current peaks. The peaks could be identified with the help of the $P(E)$-function to a single and multiphoton transitions in the environment.

Chapter 6

Peaks due to Inelastic Cooper Pair Tunneling

The purpose of this chapter is to describe the inelastic tunneling in a situation where there are one or two large SQUIDs used as an environment for the probe junction. The situation is equivalent to the one studied in chapter 3. The calculation there was purely classical but now we are dealing with a completely different phenomenon, the excitation of macroscopic quantum states. To derive the $I-V$ characteristics we use a perturbative method in the same fashion as done in the $P(E)$-theory. This situation was recently realised in the experiments and interesting phenomena were seen [14, 40, 41] interpreted as a proof of inelastic Cooper pair tunneling and the band structure of the Josephson junctions. We will analyze these experiments in more detail in chapter 7.

At first we will show how to calculate the current-voltage characteristics in the limit $s \gg 1$ using the $P(E)$-theory. After that we will analyze the matrix elements used in the perturbation theory to describe the system more generally. Then we will add another SQUID to the system and find an approximate solution. After that we will discuss the spectroscopic methods available when using SQUIDs as an environment. Finally we will discuss the influence of the gate voltage and show how the Bloch bands should be seen in the experiments.

6.1 Current Using the $P(E)$-theory

Let us assume that we have a SQUID (or equivalently a tunable Josephson junction) acting as an environment for the probe junction. If $s \gg 1$ for the SQUID, we can describe the situation with the help of the $P(E)$-theory. This is because now the SQUID acts as it would be an LC-oscillator whose impedance could written as a parallel contributions of $i\omega L$ and $\frac{1}{i\omega C_1}$, so we

have

$$Z(\omega) = \frac{1}{i\omega C_1 + \frac{1}{i\omega L}}. \tag{6.1}$$

The tunneling impedance (5.21) is now

$$Z_t(\omega) = \frac{1}{i\omega C_p + i\omega C_1 + \frac{1}{i\omega L}} = \frac{1}{i\omega C_\Sigma + \frac{1}{i\omega L}} = \frac{1}{C_\Sigma} \frac{i\omega}{\omega_p^2 - (\omega - i\epsilon)^2}, \tag{6.2}$$

where C_p is the probe's capasitance, $C_\Sigma = C_p + C_1$ and ω_p is the plasma frequency (2.21) of L and C_Σ. The tunneling impedance is now the same as in equation (5.29) except that the capasitance in (6.2) is the sum C_Σ. Peaks appear in the $I - V$ curve with a separation

$$V = \frac{\hbar\omega_p}{2e}. \tag{6.3}$$

We will from now on call this ω_p as an effective plasma frequency of the system. Usually $C_p \ll C_1$ so the plasma frequencies of the SQUID and the system won't differ a lot. Using (5.32) and (2.21) we obtain the probability density parameter

$$\rho = \frac{4E_c}{\hbar\omega_p} = \frac{4E_c}{\sqrt{8E_cE_j}} = \sqrt{\frac{2}{s_\Sigma}}, \tag{6.4}$$

where s_Σ is now the ratio of the SQUID's coupling energy and the system's charging energy (using $C = C_\Sigma$). The area of the k:th peak is as before (5.34).

6.2 Matrix Elements of the Perturbation

Let us now derive the current-voltage characteristics of the previous situation directly by a perturbative method. This analysis is needed for example when the assumption $s \gg 1$ for the SQUID is no longer valid.

First we will calculate the unperturbed Hamiltonian. The Josephson potential energy of the probe will be neglected and the probe will be described at first only by a capasitor. The Hamiltonian can be written in the form

$$H = \frac{{Q_1}^2}{2C_1} + \frac{{Q_p}^2}{2C_p} - E_1 \cos(\varphi_1). \tag{6.5}$$

We assume an ideal voltage source (could be viewed as a consequence of a large stray capasitance) so we demand that

$$\frac{Q_1}{C_1} + \frac{Q_p}{C_p} = V. \tag{6.6}$$

This says that the charges are not independent and only one charge variable is needed. We define an island charge

$$Q = Q_p - Q_1, \tag{6.7}$$

which describes the charge of the middle electrode between the capasitors. Using equations (6.5-7) we obtain [42]

$$H = \frac{Q^2}{2C_\Sigma} - E_1 \cos(\varphi_1) + \text{constant}. \tag{6.8}$$

Again, we forget the constant.

What about the phase variables φ_1 and φ_p, are they independent? No they are not. We could view that the assumption of a constant voltage results in the relation (3.8) for the total phase difference across the junctions. It is now assumed to be a classical variable, the phase difference between the macroscopic superconductors. The phase related to the island however can have quantum fluctuations.

The basis of coordinates can be choosen arbitrary and they will all lead to the same result. For this situation it is conventional to identify that $-\varphi_1$ (rather than φ because Q_1 has a negative contribution in equation (6.7)) is the conjugated variable to the island charge and mark $-\varphi_1 = \varphi$, leading to the relation

$$[\varphi, Q] = 2ei. \tag{6.9}$$

Usually it is chosen that $\varphi = \frac{1}{2}(\varphi_2 - \varphi_1)$ but at the end, after a similar change of variables as done in section 5.2, we would be dealing with exactly the same equations than with this choice of basis. The exact derivation of the correct variables should be done by starting from the Lagrangian function under a voltage bias, but it is not presented here. The Hamiltonian (6.8) becomes now similar as in (4.9) and the eigenfunctions are therefore the Bloch wave functions (4.10-12).

We assume that the current can be calculated with the help of the transition rates, as done in chapter 5: the excited state must have a short lifetime compared to the tunneling rate. The perturbation for a positive sign current is

$$H_t = -\frac{E_p}{2} e^{-i\varphi_2} = -\frac{E_p}{2} e^{-i(\frac{2eV}{\hbar}t + \varphi)}. \tag{6.10}$$

The perturbation is harmonic ($e^{-i\omega t}$ dependence) so it induces an absorbtion $2eV$ of energy to the unperturbed system, corresponding to a Cooper pair tunneling. The transition amplitude from the state i to f is obtained from

$$A_{i\to f} = -\frac{E_p}{2} \langle f | e^{-i\varphi} | i \rangle, \tag{6.11}$$

which describes an excitation of the unperturbed system from the state i to f. The transition rates are

$$\Gamma^{\pm}(V) = \frac{\pi {E_p}^2}{2\hbar} \sum_f \sum_i P_\beta(i) |\langle f|e^{\mp i\varphi}|i\rangle|^2 \delta(E_f - E_i \mp 2eV). \tag{6.12}$$

The current is found as before (5.19). We see that the matrix elements are similar as in the $P(E)$-theory derived in chapter 5. However, the basic states are no longer just the harmonic oscillator's eigenstates, they are generally the Bloch eigenstates with a quasicharge q. The quasicharge is now interpreted to be the charge which is given to the middle electrode and without any doping this is always zero. Also the perturbation doesn't change q (equivalent to that the Josephson tunneling won't change the quasicharge) and therefore the initial and the final states don't have to be summed over different values of the quasicharge. All the matrix elements with differing quasicharges vanish. We could write equivalently

$$\Gamma^{\pm}(V) = \frac{\pi {E_p}^2}{2\hbar} \sum_{n_f,q} \sum_{n_i,q} P_\beta(n_i,q) |\langle n_f,q|e^{\mp i\varphi}|n_i,q\rangle|^2 \delta(E_{n_f,q} - E_{n_i,q} \mp 2eV). \tag{6.13}$$

The probability distribution can contain many different values for q if the state is for some reason changing in time. Then $P_\beta(n,q)$ gives the probability that the island has the quasicharge q and is in the n:th energy band. The quasicharge dependence is discussed in more detail in sections (6.5) and (6.6). For simplicity we won't usually mark explicitely the quasicharge of the states.

Using the approximation $T \approx 0$ we can identify the $P(E)$-function from (6.12)

$$P(E) = \sum_f |\langle f|e^{-i\varphi}|0\rangle|^2 \delta(E_f - E_0 - E). \tag{6.14}$$

The peaks are now infinitely high because no dissipation is taken account (a possible resistance of the leads). A small dissipation will broaden the resonances and is described by replacing the δ-function by a Lorenzian curve

$$\delta(E_f - E_0 - E) \to \frac{2}{\pi} \frac{\Delta_f}{4(E_f - E_0 - E)^2 + {\Delta_f}^2}, \tag{6.15}$$

where Δ_f is the line width of the final state's energy level. The area of the peak (6.15) is still unity. Using equations (6.14) and (6.15) we obtain

$$P(E) = \frac{2}{\pi} \sum_f |\langle f|e^{-i\varphi}|0\rangle|^2 \frac{\Delta_f}{4(E_f - E_0 - E)^2 + {\Delta_f}^2}. \tag{6.16}$$

If $s \gg 1$ we should obtain the $P(E)$-theory's LC-oscillator model, derived in section 6.1. This can be shown directly by approximating the Bloch wave functions locally as harmonic oscillator's eiqenfunctions. These are in the Josephson junction "language"

$$\psi_n(\varphi) = N_n \mathrm{He}_n(y) e^{-\frac{1}{2}y^2} \tag{6.17}$$

$$y = \left(\frac{s_\Sigma}{8}\right)^{\frac{1}{4}} \varphi = \alpha\varphi \tag{6.18}$$

$$N_n = \left(\frac{s_\Sigma}{8\pi^2}\right)^{\frac{1}{8}} \sqrt{\frac{1}{2^n n!}}, \tag{6.19}$$

where He_n is the n:th Hermite's polynome. For the few first n values these are

$$\mathrm{He}_0(y) = 1 \tag{6.20}$$

$$\mathrm{He}_1(y) = 2y \tag{6.21}$$

$$\mathrm{He}_2(y) = 4y^2 - 2 \tag{6.22}$$

$$\mathrm{He}_3(y) = 8y^3 - 12y. \tag{6.23}$$

Now we can calculate the transition amplitudes, for example

$$\begin{aligned} A_{0\to 0} = \langle 0|e^{-i\varphi}|0\rangle &= \left(\frac{s_\Sigma}{8\pi^2}\right)^{\frac{1}{4}} \int_{-\infty}^{\infty} e^{-y^2} e^{-i\varphi} d\varphi \\ &= \left(\frac{s_\Sigma}{8\pi^2}\right)^{\frac{1}{4}} \int_{-\infty}^{\infty} e^{-\alpha^2\varphi^2} (\cos(\varphi) - i\sin(\varphi)) d\varphi \\ &= 2\left(\frac{s_\Sigma}{8}\right)^{\frac{1}{4}} \int_0^{\infty} e^{-\sqrt{\frac{s_\Sigma}{8}}\varphi^2} \cos(\varphi) d\varphi. \end{aligned} \tag{6.24}$$

The $P(E)$-theory stated that the k:th peak has the area ρ_k. This leads to the demand

$$\rho_k = |A_{0\to k}|^2. \tag{6.25}$$

Calculating the transition amplitudes numerically one sees that indeed they give the same result as using (6.4) and (5.34).

6.3 Double SQUID Environment

In experimental situations there can be many SQUIDs placed around the probe to obtain a better control of the experiment. We want to know if the theory is valid in this situation also. Let us now consider the configuration shown in figure 6.1, two SQUIDs are placed on the different sides of the probe junction and the circuit is voltage biased.

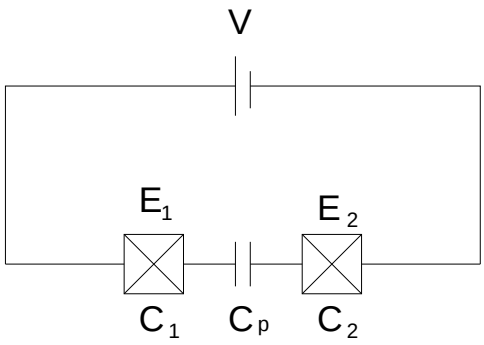

Figure 6.1: Two SQUIDs at the different sides of the probe junction.

We calculate the current in the same fashion as done before. The Josephson potential energy of the probe junction will be included by a perturbative method. The assumption of an ideal voltage source leads to

$$\frac{Q_1}{C_1} + \frac{Q_2}{C_2} + \frac{Q_p}{C_p} = V. \tag{6.26}$$

We now define the left and the right island charges

$$Q_p - Q_1 = Q_L \tag{6.27}$$
$$Q_2 - Q_p = Q_R, \tag{6.28}$$

and obtain for the unperturbed Hamiltonian

$$\begin{aligned} H = &- E_1 \cos(\varphi_1) - E_2 \cos(\varphi_2) + \frac{{Q_L}^2}{2(C_1 + C_{23})} \\ &+ \frac{{Q_R}^2}{2(C_{12} + C_3)} + \frac{Q_L Q_R C_{123}}{C_1 C_3} + \text{constant}, \end{aligned} \tag{6.29}$$

where $C_{ij} = \left(\frac{1}{C_i} + \frac{1}{C_j}\right)^{-1}$ and $C_{ijk} = \left(\frac{1}{C_i} + \frac{1}{C_j} + \frac{1}{C_k}\right)^{-1}$. Let us assume that $C_p \ll C_1$,C_2. This is probably true because the probe junction usually the smallest from its dimensions (to have a small Josephson couling energy). Then we can eliminate the second last term in (6.29) and obtain (by neglecting the constant)

$$H = -E_1 \cos(\varphi_1) - E_2 \cos(\varphi_2) + \frac{{Q_L}^2}{2(C_1 + C_p)} + \frac{{Q_R}^2}{2(C_p + C_3)}. \tag{6.30}$$

We can now interpret that $-\varphi_1$ and Q_L are conjugated variables and the same is true for φ_2 and Q_R. But $-\varphi_1$ and Q_R do commutate and are independent operators as are φ_2 and Q_L. This could be viewed that we have two particles, the left and the right one, which do usually have a coupling

described by the second last term in the Hamiltonian (6.29), but in this situation it is vanishing.

The Hamiltonian (6.30) consist of two independent parts

$$H_L = -E_1 \cos(\varphi_L) + \frac{{Q_L}^2}{2(C_1 + C_p)} \tag{6.31}$$

$$H_R = -E_2 \cos(\varphi_R) + \frac{{Q_R}^2}{2(C_p + C_3)}. \tag{6.32}$$

The total Hamiltonian's eigenstates are therefore products from the eigenstates of these two subspaces. We obtain

$$|i\rangle = |i_L\rangle |i_R\rangle. \tag{6.33}$$

The perturbation contributing to the positive sign current can be written in the form

$$-\frac{E_p}{2} e^{-i\varphi_2} = -\frac{E_p}{2} e^{-i(\frac{2eV}{\hbar} + \varphi_L - \varphi_R)}. \tag{6.34}$$

The transition rates can be written in the form

$$\begin{aligned} \Gamma^{\pm}(V) = & \frac{\pi {E_p}^2}{2\hbar} \sum_{f_L} \sum_{i_L} \sum_{f_R} \sum_{i_R} P_\beta(i_L) P_\beta(i_R) |\langle f_L | e^{\mp i\varphi_L} | i_L \rangle \\ & \langle f_R | e^{\pm i\varphi_R} | i_R \rangle|^2 \delta(E_{f_L} + E_{f_R} - E_{i_L} - E_{i_R} \mp 2eV). \end{aligned} \tag{6.35}$$

The matrix elements aren't dependent on the sign of the exponent $e^{\mp i\varphi}$, therefore we see that the main resonances occur when either the left or the right island stays in its ground state and the other is excoted. This gives resonances exactly at the same positions as in the previous situation. But, there are also multiphoton prosesses where both of the islands are exciting.

If the SQUIDs are identical, $s \gg 1$ and $T = 0$ the effect of the double SQUID environment is easy to evaluate. For example, when calculating the transition rate for the second peak (the first harmonic), one has to take into account the contributions from that either the left or the right island excites two quanta and the other one stays in the ground state, but also the possibility that both the islands excite one quantum. This is the same thing as we had two independent resonances in the $P(E)$-theory, as discussed in section (5.6), but now with the same plasma frequencies. This will double the tunneling impedance (5.21) leading to

$$\rho = \sqrt{\frac{8}{s_\Sigma}}, \tag{6.36}$$

which is double the value (6.4) obtained from the single SQUID calculation. In a general situation however, the energy states are not equally spaced and

new peaks should appear due to multiphoton transitions. This is because, for example, the transition where either the left or the right island excites two quanta needs a different energy than the transition where both of the islands excite one quantum.

If the second last term in equation (6.29) wouldn't be vanishing, it would introduce a coupling between the two islands. We could take it into account by using the time independent perturbation theory and it would lead to an interesting effect: the degeneracy of the energy states would vanish and the energy levels should split. If however $C_1, C_2 \gg C_p$, this effect is very small.

6.4 Spectroscopy when using SQUID as an Environment

The reason why SQUIDs, rather than Josephson junctions, are exellent tools for a spectrometry in these kind of systems is that we can change the Josephson coupling energy of the SQUIDs by applying a magnetic field to the system, as shown in equation (2.28). This results in a different coupling of the probe junction to the environment as measured in Refs. [43, 44]. In our case of interest, the magnetic flux moves the resonances in the current-voltage characteristics, if the resonances won't move, they aren't coming from the SQUID.

Usually $s \gg 10$ and the relative magnitude of the peaks decreases very rapidly, as can be seen from equations (6.4) and (5.34). However, decreasing s by increasing the magnetic field, the harmonics should arise comparing to the fundamental resonance. This is a good way to test the theory.

If our circuit consist of a SQUID and some arbitrary oscillator with a smaller plasma frequency, extra peaks will show up nearby the resonances of the SQUID due to multiphoton transitions, as discussed in section 5.6. When applying a magnetic field, the main resonances will move, taking the multiphoton transitions with them. But the multiphoton transition will stay at a constant distance from the peaks, implying that the nearby transition isn't coming from the SQUID; if it were, the distance shouldn't be a constant. Therefore one can trace very effectively from where each of the peaks is coming.

6.5 Voltage Biased Superconducting Single Electron Transistor

We can introduce an external coupling to the two Josephson junction system by adding a gate voltage to the island as shown in figure 6.3, the system is called a voltage biased Superconducting Single Electron Transistor (SSET).

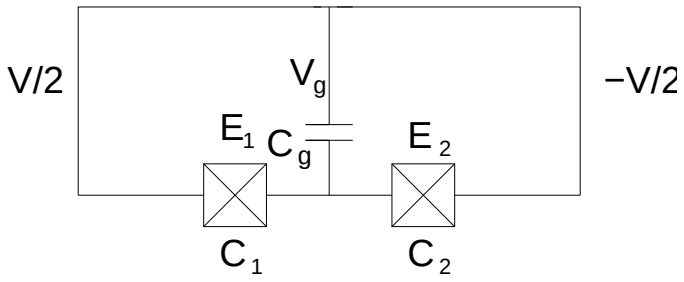

Figure 6.2: A voltage biased SSET. The gate voltage V_g is coupled to the island by a capasitance C_g.

Let us analyze the effect of the gate voltage when $V = 0$. After a similar calculation than done in section 6.2, we would obtain the Coulomb energy of the system is

$$U = \frac{Q^2}{2C_\Sigma}, \tag{6.37}$$

where $C_\Sigma = C_1 + C_2 + C_g$ and Q is the island charge. However, this isn't the potential energy which determines the energy change in the circuit after a tunneling event. For example if we had a voltage biased single junction, the energy change of the Coulomb energy is zero (Q is a constant), but there is $2eV$ energy gain due to external work done by the voltage sources. In this situation, the work done by the voltage sources when n Cooper pairs tunnel from the lead j to the island can be written in a form [30]

$$W_j = -n2e\sum_i (V_j - V_i)\frac{C_i}{C_\Sigma}. \tag{6.38}$$

One sees that generally this depends on which of the leads the Cooper pair is coming and therefore introduces problems when writing the Hamiltonian.

Assuming that $V_1 = V_2 = 0$ we obtain an unique value for the Hamiltonian (substracting (6.38) from the usual contribution of the two Josephson junctions)

$$H = -E_1\cos(\varphi_1) - E_2\cos(\varphi_2) + \frac{(Q - Q_0)^2}{2C_\Sigma}, \tag{6.39}$$

where $Q_0 = -V_g C_g$ is the gate charge. Because $V = 0$ the overall phase difference φ_Σ is some constant c. Thus equation (6.39) can be rewritten in

the form

$$H = -E_j(c)\cos(\varphi - \eta) + \frac{(Q - Q_0)^2}{2C_\Sigma} \tag{6.40}$$

$$E_j(c) = \sqrt{({E_1}^2 + {E_2}^2 + 2E_1E_2\cos(c))} \tag{6.41}$$

$$\varphi = \frac{1}{2}(\varphi_2 - \varphi_1) \tag{6.42}$$

$$\eta = \tan^{-1}[\frac{E_1 - E_2}{E_1 + E_2}\tan\left(\frac{c}{2}\right)]. \tag{6.43}$$

We see that if $V = 0$, then the SSET acts as a single Josephson junction with an adjustable island charge. This is the situation discussed in section 4.4, the change of the gate charge is now our doping mechanism an it corresponds to a change of the quasicharge in the eigenstate. We have now an external control of the quasicharge. However, in practice, random charged impurities near the island may shift the effective gate charge by an amount of Q_{00}. This change is independent on V_g but may drift continuously or discontinuously in time, killing our precise control of the gate charge. Taking this effect into account we define

$$Q_0 = -C_gV_g + Q_{00}. \tag{6.44}$$

When $V \neq 0$, the situation is no more so simple. The phase difference between the leads starts to travel in time leading to a time dependent Hamiltonian. A new term will appear into equation (6.39) which will describe the energy gain when a charge has gone through the circuit. To describe a non-vanishing current, we have to take into account the dissipation as discussed in section 5.1. The experimental and the theoretical work of this kind of systems has been active [45, 46, 47, 48] and usually they are done when quasiparticles are present in the island leading to e or $2e$ periodic dependence of the current as a function of the gate charge. The difference in characteristics between the cases when there is an even or odd number of electrons in the island, is called the parity effect.

6.6 Effect of the Gate Voltage to Inelastic Cooper Pair Tunneling

Our system in study is very analogous to the cases studied in Refs. [45, 46, 47, 48]. The main difference is that we have no quasiparticle excitations and we are treating one junction as a perturbation to the other. The role of the gate charge is also a little bit different, we aim that a change in the voltage will result in a change in the Bloch wave function. We add a gate voltage to this system in the same way as done in section 6.5 and using (6.38) obtain

for the unperturbed Hamiltonian

$$\begin{aligned} H &= -E_1\cos(\varphi) + \frac{Q^2}{2C_\Sigma} - \frac{Q}{C_\Sigma}(C_pV + C_gV_g') \\ &= -E_1\cos(\varphi) + \frac{(Q-Q_0)^2}{2C_\Sigma} + \text{constant}, \end{aligned} \tag{6.45}$$

where we have defined $Q_0 = C_pV + C_gV_g'$, $V_g' = \frac{V}{2} - V_g$ and $-\varphi_1 = \varphi$. Again, we can manipulate the unperturbed Hamiltonian by the gate voltage which changes the gate charge resulting in a change of the quasicharge. The gate charge is a function of the gate voltage but also of the voltage between the leads. We actually didn't take this extra contribution into account in sections 6.2 and 6.3, where it should be present but acting as a constant (corresponds to case $C_g = 0$ in this model). One should note that again Q_0 contains also the effect of the impurities as defined in equation (6.44). This might partly decrease the total external control of the gate charge.

We use the perturbation (6.10) and obtain the same $P(E)$-function as in equation (6.16) when $T \approx 0$. The situation is now however different, we have the control of the quasicharge and we can manipulate it by using the gate voltage. Therefore we can access the $P(E)$'s quasicharge dependence. Normally when dealing in the region $s \gg 1$, this doesn't bring any changes to the lowest resonances but the higher bands may be dependent on the quasicharge, as seen in figure 4.1. The gate charge will affect the inelastic Cooper pair tunneling into these bands. Changing the gate voltage, we change the energy of the excited state and therefore the position of the resonance in the $I-V$ curve. Also the transition amplitude is changed and the height of the peak may rise or lower. The effect will become more and more evident when decreasing the Josephson coupling energy of the SQUID finally leading to a band structure even in the lowest energy states.

In figure 6.3 are plotted the numerical results for the transition probabilities from the first band to the fourth band as a function of $s = \frac{E_j}{E_c}$. The probabilities were calculated for two cases, when $q = 0$ and $q = e$, using the corresponding Mathieu functions [49] as wave functions of the island. At these special points they are 2π or 4π periodic, so the matrix elements could be calculated locally (for example by integrating from 0 to 4π). The perturbation doesn't change the quasicharge so only the transition $|0,q\rangle \to |3,q\rangle$ has to be calculated. For comparison, figure 6.3 also shows the corresponding transition probability of the harmonic oscillator.

6.7 Validity of the Model

The model is derived using the probe junction as a perturbation and clearly in some limit it won't be valid anymore. Heuristically we could say that E_p has to be small, smaller than the other elements in equation (6.8) and

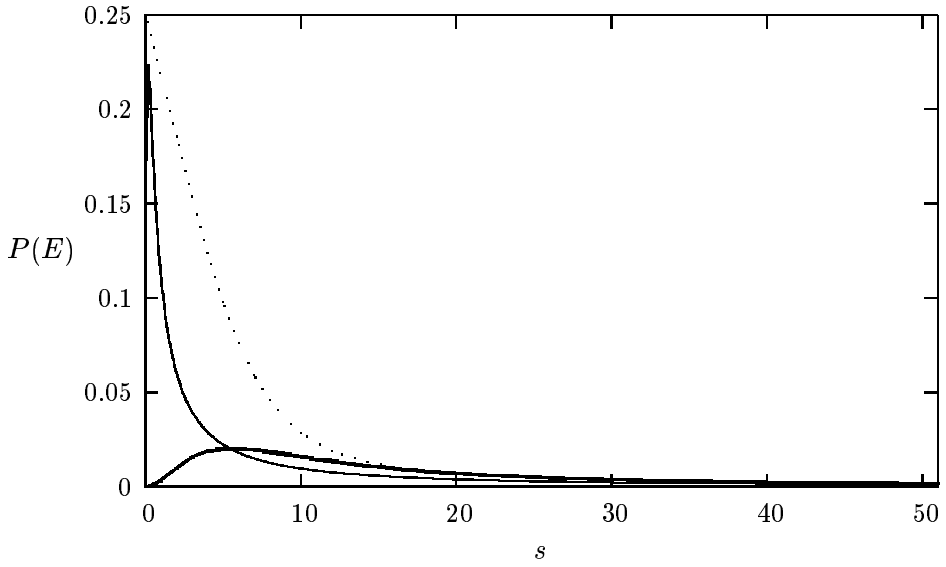

Figure 6.3: Numerical results for the transition probabilities to the fourth band as a function of the Josephson coupling energy. The three curves correspond to the coupling when $q = e$ (the dotted curve), $q = 0$ (the solid line, vansishes when $s = 0$) and when the system is a harmonic oscillator (the solid line, doesn't vanish when $s = 0$). The curves approach each other when $s \to \infty$. However, when $s = 50$ the couplings between the Bloch wave functions are a half larger than between the harmonic oscillator's eigenfunctions.

our theory is correct. Calculating the second order amplitudes for the time dependent perturbation theory, one could argue that it is sufficient that $E_p \ll E_1$ even $E_p > E_c$ in the situation $s \gg 1$. We have to take into account also the relaxation to the ground state. If the damping isn't high enough, the excited states might not relax to the ground state fast enough and the model won't hold. Now the basic states could even be formed from the collective behaviour of the two SQUIDs, as in the SSETs generally. Then the assumption that the current obeys the transition rate calculus may fail before the perturbation theory even diverges.

It is also important to notice that the important relative magnitudes of the energy won't usually have any information of the probe's capasitance. The probe's charging energy might be huge because of its small capasitance, but what is important, is the charging energy of the island, obtained by using the sum of all capasitances C_Σ. The charging energy of the island might be an order of magnitude smaller than the probe's charging energy.

Chapter 7

Comparison with the Experimental Data

In this chapter we will compare the two models introduced in chapters 3 and 6 and see how do they differ in $I-V$ characteristics. After that we will discuss the experiments done by R. Lindell *et. al.* for mesoscopic junctions and see which model, if any, is valid for those cases. Finally we will discuss the Bloch bands which were interpreted to be seen in these experiments.

7.1 Comparison Between the Models

We derived two models (chapters 3 and 6) for many Josephson junction systems in a situation where the junctions differ essentially in size. The first one described a classical movement of the phase differences in the presence of a quasiparticle current and possible high frequency lead impedance. The second one described excitations of the quantum states using a probe junction as a perturbation source. They manifest completely different physics but still similar $I-V$ curves were obtained. The classical model was possible only when taking into account a dissipation mechanism, the system has to dissipate the energy gained from the voltage source. In the quantum mechanical treatment the dissipation was also necessary. It takes care of that the system is in its ground state before the next tunneling and takes the energy gained from the tunneling of one Cooper pair.

The two models gave rise to peaks at the same positions in the $I-V$ curve in the limit $s \gg 1$. Why? Because both of the models include the same important frequencies, the plasma frequency of the larger junction (or the plasma frequency of the system) and the quantum mechanical time evolution of the phase difference across the probe junction. In the classical treatment these two frequencies are in a resonance when the current peak occurs. In the latter treatment the probe introduces a perturbation which leads to transitions between the harmonic oscillator's eigenstates which differ

in energy by multiples of the plasma frequency times $\hbar$. This leads to a current at certain voltages, the same ones as in the classical case.

However, the shape of the peaks differ greatly. The classical model reacts more easily to the anharmonic nature of the Josephson potential energy, leading to a hysteretic behaviour and a shift of the peaks. The quantum excitations result in more symmetric curves, even when the anharmonicity of the Josephson potential becomes crucial. The sinusoidal shape results in closer resonances at the voltage axis at higher voltages (compared to the harmonic oscillator approximation) and finally leads to a quasicharge dependence of the energy and the current. An important difference was also that the classical model didn't give rise to the second or higher harmonics. This could be due to our choice of parameters, they might be present in other situations. This is however the clearest difference between the models when using the parameters of our interest.

7.2 Comparison with the Experiments

We will now apply our models to two recent experiments made by R. Lindell *et. al.* [14, 41] in an analogous double SQUID situation as discussed in chapter 6. The two identical SQUIDs consisted of mesoscopic Josephson junctions and the Josephson coupling energy and capasitance of the probe junction were small compared to the other elements in the system. Also, in one of the two experiments [14] the SQUIDs' coupling energies were tuned (with the help of the magnetic field) in the region $s \in [50 \rightarrow 10]$ so the Bloch band structure could also be studied. The temperature in the experiments was $k_B T \approx 7\ \mu eV$ which was on the order of magnitude less than $\hbar\omega_p$, so to simplify modelling we can assume that $T = 0$. E_c of the system was in the range $7 - 10\ \mu eV$ and therefore (4.3) is not satisfied. However, we are not observing single charging effects, the relevant energy prosesses of the inelastic tunneling are in the range $200\ \mu eV$ and this is not a problem for that. But one could discuss if the band structure of the Bloch wave functions suffer from the high temperature.

Figure 7.1 shows the experimental and theoretical $I - V$ curves for the experiment done in Ref. [41]. The experimental $I - V$ curve is only an approximation from the original, we have omitted all the fine structure which was present in the main resonances and concentrate only on the overall behaviour. Also the supercurrent behaviour ($V \approx 0$) is not included. The quantum mechanical $I - V$ curve is calculated by using the harmonic oscillator's wave functions as the basic states of the system and they lead to the value (6.36) for the probability parameter describing the heights of the peaks (5.34). The classical $I - V$ curve is calculated by using a two SQUID environment for the probe junction, the calculation is described in section 3.7. The values for the parameters of the junctions are obtained from the

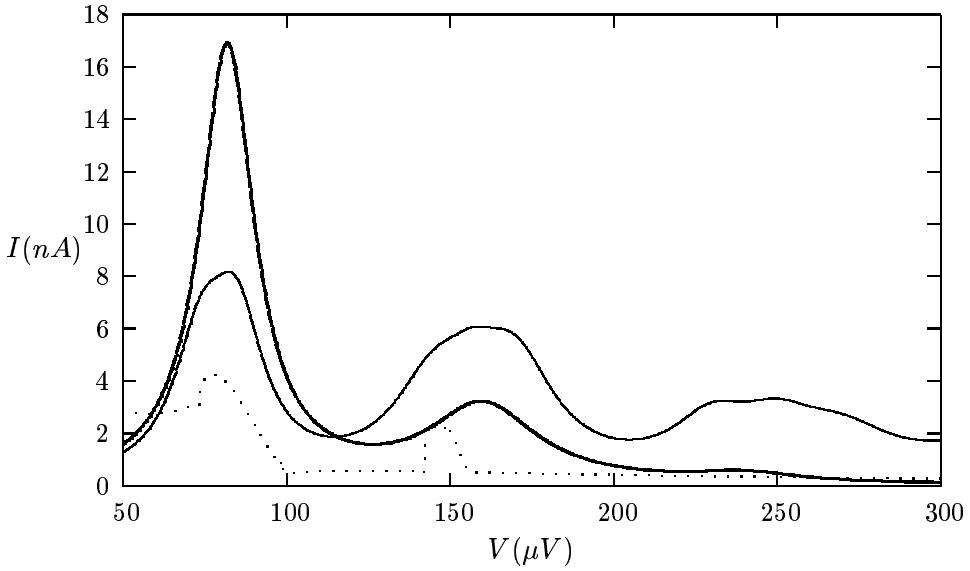

Figure 7.1: The experimental and theoretical $I-V$ curves for the experiment done in Ref. [41]. The dotted curve corresponds to the classical calculation, the solid line which is the highest when $V = 80\ \mu V$ correspond to the quantum mechanical calculation and the solid line which is the highest when $V = 300\ \mu V$ corresponds to the experimental curve. In the classical calculation we used $\hbar\omega_p = 2 \times 80\ \mu eV$, $G_1 = G_3 = 1\ \frac{\mu}{\Omega}$ (SQUIDs), $G_2 = 0.1\ \frac{\mu}{\Omega}$ and $R = 250\ \Omega$.

normal state behaviour of the system but have to be partly fitted to obtain a better agreement with the experiments. The value for the SQUID's Josephson coupling energy, $\approx 2 \times 74\ \mu eV$, is obtained from equation (2.9) and is almost the same whether using the correction (4.29) or not. However, we use a value $\hbar\omega_p = 2 \times 82 \mu eV$ by increasing the Josephson coupling energy of the SQUIDs by approximately 23 percent, which does match to the experimental value seen in figure 7.1. The precise value of E_p is also unknown but we used the value obtained from equation (2.9), the "correction" (4.29) would give way too small value for the observed currents. The line widths in equation (6.15) are obtained from the experimental curve. Only region $0 \leq V \leq 400\ \mu V$ is available for the experimental studies since aluminum's gap function has the value $\approx \Delta = 200\mu\ eV$ and beyond $\frac{2\Delta}{e}$ the quasiparticle tunneling takes a dominant part of the tunneling prosesses.

From figure 7.1 we see that the curves somehow do fit in the peak positions but not in the heights. The harmonics are strong compared to the fundamental resonance in the experimental curve and this is not the case for the theoretical calculations. The classical calculation gives a strong first

harmonic but there are no second one which is clearly present in the experimental data. The quantum mechanical calculation gives the latter peaks but the heights of the harmonics are low.

Could we obtain stronger harmonics by changing the parameters? The classical calculation doesn't give the second harmonic for any reasonable values of the parameters. In the quantum mechanical calculation increasing E_p won't help anything because it won't change the relative heights of the peaks. However, changing E_1 the latter peaks can be made higher but then the positions of the peaks will be in disagreement with the experiments. This could be corrected by changing the capasitance of the SQUID but now the fitting starts to go unsound, the measured capasitance should be quite correct and we are no longer really describing the original system. Therefore we cannot explain the behaviour exactly by neither of the models.

One could think that the existense of the second harmonic points to the quantum mechanical behaviour and the theory of inelastic Cooper pair tunneling. We can only quess why the simple model in chapter 6 won't hold for this experiment. In the experiment the coupling energy (2.9) of the probe was approximately 56 μeV and the effective plasma frequency 2×80 μeV. Mayby the transition rate calculus starts to be in the region where it is no longer valid, the coupling energy of the probe is too strong. One can ask whether the probe junction now only a small perturbation, or is it also a part of the collective state of the SSET.

Let us now concentrate on the experiment done in Ref. [14] which is similar to the first one but now with slightly different parameters for the Josephson junctions. In figure 7.2a is shown the experimental $I-V$ curve and in figure 7.2b the theoretical $I-V$ curve of the quantum mechanical calculation. The theoretical curve is calculated numerically using the Mathieu functions as the basic states of the system. The current can be calculated with the help of the couplings between the different bands using equations (6.35) and (5.19). We are in the limit $s \approx 50$ so the tunneling rates are independent of the quasicharge and the energy bands are practically energy levels. However, the energy levels are no longer equally spaced because of the anharmonic nature of the Josephson potential energy (we didn't take this effect into account when modelling the first experiment because the line widths there were so large that they masked this effect). Independent experiments for the Josephson coupling energies of the SQUIDs pointed that $\hbar\omega_p \approx 2 \times 103.7$ μeV as used in chapter 3. This experimental value was double the value which would have been obtained from the normal state behaviour using equation (2.9). The correction (4.29) didn't explain this change. However, we still manipulate the value of E_j about 6 percent to lower the effective plasma frequency from 2×103.7 μeV to 2×100.7 μeV and obtain a better fit. The effective charging energy was $E_c \approx 9.9$ μeV and the probe's coupling energy is approximated to be 3.6 μeV. The linewidths were adjusted to be similar as in the experimental curve 7.2a.

Figure 7.2a

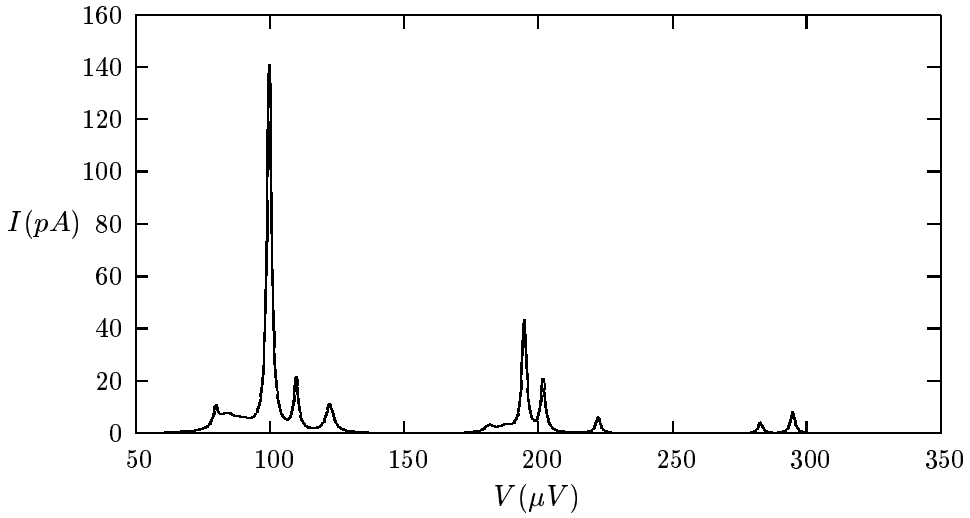

Figure 7.2b

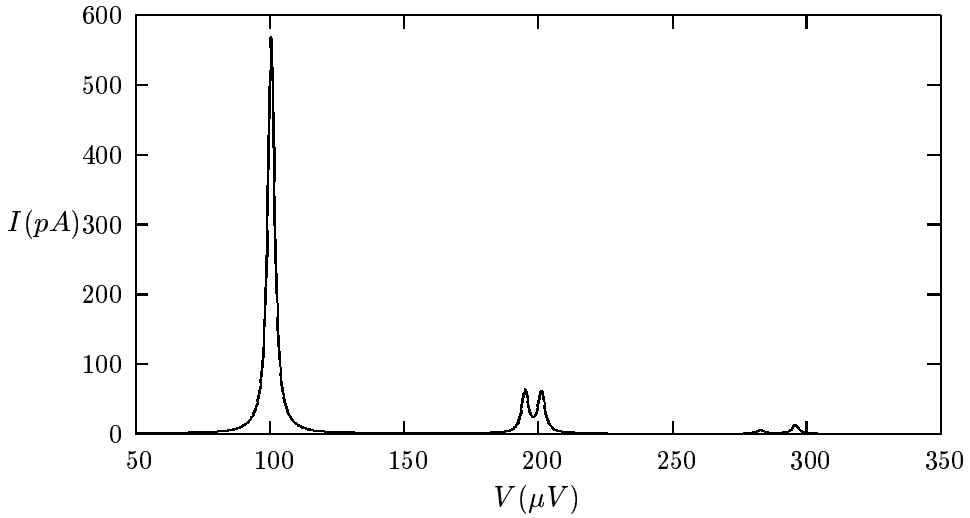

Figure 7.2: The experimental (figure 7.2a) and quantum theoretical (figure 7.2b) $I-V$ curves of the experiment done in Ref. [14]. Notice the different scales of the current axises.

In the experimental curve there is a multiple peak structure present nearby the main resonances. The quantum theoretical curve is close to the experimental when neglegting the relative heights but few peaks are missing. The douple peak structure for harmonics in the theoretical calculation is formed from the multiphoton transitions into the two SQUIDs and taking into account that the energy level separations aren't constant as in the case of the harmonic oscillator. Especially the double peak at 290 μV is in a good agreement with the energies of the Bloch bands.

Approximately at $V = 10\ \mu V$ (not shown in figure 7.2a) there is a peak in the experimental data probably due to external oscillator. The peak at $V \approx 110\ \mu V$ could be a multiphoton transition to this. The peak nearby $V \approx 123\ \mu V$ is identified to be the fundamental resonance of another external oscillator (doesn't react to the magnetic field) and the multiphoton transition with this and the SQUID is at $V \approx 223\ \mu V$. The peak in $V \approx 202\ \mu V$ cannot be the multiphoton transition with the SQUID and the smaller external oscillator because it is at a wrong distance from the main resonance and the height of the multiphoton transition should actually be vanishing (so we can interpretate that this peak comes from the SQUIDs, as in figure 7.2b). By taking into account these two new oscillators into our theory, the corresponding $I - V$ curve would be in a good agreement with the experimental positions of the peaks. However, there would be still a small unexplained asymmetric behaviour on the left sides of the first two resonances, as seen in figure 7.2a as small peaks at the positions $\approx 80\ \mu V$ and $\approx 180\ \mu V$. These cannot be due to multiphoton transitions since they should be at the right sides of the main resonances at $T = 0$.

Figure 7.3 shows numerical results for the classical $I - V$ curve using the two SQUID model and the same junction parameters as in the quantum mechanical calculation. The resistance was assumed to be 250 Ω and the quasiparticle conductances almost vanishing $G_1 = G_3 = 0.5\ \frac{\mu}{\Omega}$, $G_2 = 0.05\ \frac{\mu}{\Omega}$. The solution becomes hysteretic near the two resonances but not as strongly as in the corresponding single SQUID calculation shown in figure 3.5. Again, only the first harmonic is found in contrast to the observation in the experiments. Also the extra peaks nearby the main resonances in the experimental data cannot be explained by the classical model.

Even though the quantum mechanical and experimental curves do fit in the peak positions, it may be that this model has just been very lucky for the following reasons. Firstly, for many samples, resonances seemed to consist from double peaks as in figure 7.2a and the two peaks were approximately at a constant distance from each other when applying a magnetic field (these constants aren't the same for every double peak). This isn't a problem for the first resonance, the multiphoton transition should stay at a constant distance from the SQUID's resonance. However, the distances obtained from the Bloch band structure (which determine the double peak structure for the harmonics as in figure 7.2b) should change a little when changing

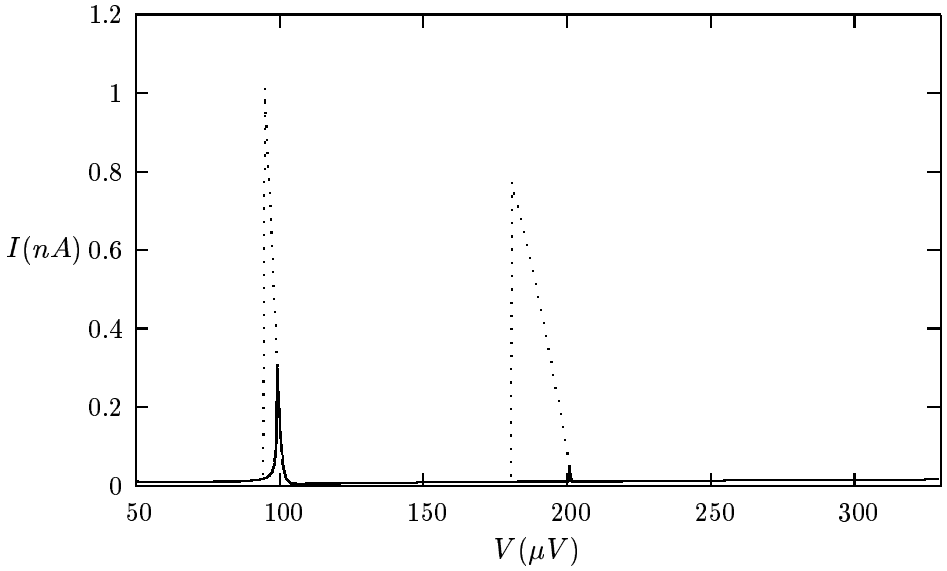

Figure 7.3: The classical $I - V$ curve of the experiment done in Ref. [14]. The dotted curve corresponds to the solution with decreasing V and the solid line correspond to the solution with increasing V.

s. For example one can calculate numerically that when s is tuned from 50 to 25 the distance of the second douple peak structure should change from $6.1\mu V$ to 6.8 μV. The third distance changes approximately from 13 μV to 15.5 μV. This change is mayby too high and probably not seen in the experiments. Secondly, the douple peaks for harmonics are present even at the one SQUID samples and theoretically this shouldn't be true at all (the double peak structure comes from the multiphoton transitions between the two SQUIDs)! It would be only possible if the down relaxation from the excited states is very slow or they are partly filled for some other reason. This kind of behaviour might also explain the peaks located at 80 μV and 180 μV.

The theoretical curve in figure 7.2b has still the same problem as before, the heights of the latter peaks are too low when comparing to the fundamental resonance. However, this effect is now much more tolerable than in the previous case: also the experimental harmonics are low. Whether the double SQUID model is correct or not, it is clear that the peaks manifest excitations of the sinusoidal potential's eigenstates and the down tuning of the third resonance is the clearest manifestation of this.

7.3 Bloch Bands

In the experiment done in Ref. [14] also Bloch bands were studied. A magnetic field was applied until the SQUIDs were in the region $s \sim 10$ and new peaks seen were interpreted to be a result of the coupling between the Bloch bands. The gate voltage didn't have any effect on the $I - V$ curve, unlike derived in section 6.6. This would actually be true if the quasicharge would have a permanent motion as in the Bloch oscillation. The edges would be highlighted and a single peak would split into two nearby peaks with different heights, as a result of different coupling from the edges $q = 0$ and $q = e$ as shown in figure 6.3. The gate voltage wouldn't have any effect because the $I - V$ curve would be a certain kind of sum of all the possible values for the quasicharge.

However, according to the model derived in chapter 6, the Bloch oscillation cannot be the answer. This is because the system is voltage biased and the Bloch oscillation is phenomenon for a current biased system. Also, the relevant charge-variable is the island charge which can be modified (theoretically) only by a Josephson tunneling across insulator (won't change the quasicharge) or by a gate voltage. Only impurities can change the effective gate charge and lead to the drift of the quasicharge. A continuous steady movement of this is not plausible and a change of the gate voltage should somehow be seen as a change of the current.

Because there are lot of peaks which probably cannot be explained by the theory already in figure 7.2a, it is very likely that these new peaks seen in the region $s \sim 10$ are not from the Bloch band structure, or at least they could be an effect of something else. When increasing the magnetic field, the energy levels will become closer to each other and also the stuff around the peaks will close each other. In the limit when Bloch band should be seen many of these extra peaks lie nearby each other and plausible identification cannot be made. However, if the gate voltage would move these peaks, it would be a great help for the identification. It should also be noted that when going to the region $E_j \sim E_c$ the perturbation theory will be less and less valid and new effects can occur only because of this.

The Bloch band structure is verified experimentally to be present in the Josephson junctions, for example, by observation of the Bloch wave oscillations. The inelastic Cooper pair tunneling is a method which should be able to reveal the band structure even more directly. And mayby it is already seen but the simplifying model of the experiments is incorrect. As a summary one could say that the eigenstates of a cosine potential are probably observed and therefore the quantum behaviour is evident. The reduction of the third peak's position is a good evidence for this. However, the collective state between the local minima of the Josephson potential (which leads to the band structure) cannot be identified. The height of the resonances is also a problem when modelling the situation with a simple model derived in

chapter 6. To describe the experimental situation better, one should mayby use a more specific analysis of the dissipative prosesses, the relaxation and the collective state of the SSET. Also the high temperature compared to the charging energy needs to be analyzed.

Chapter 8

Discussion

The purpose of this master's thesis was to analyze the current-voltage peaks which arise in the voltage biased many (mesoscopic) Josephson junction systems. Especially we studied the situations where there were one junction with small Josephson coupling energy and one or two identical SQUIDs with large Josephson coupling energies in series with the voltage source. The analysis was made for both the semiclassical and the quantum mechanical situations.

The first part of the thesis showed that peaks observed in the experiments, spaced by the plasma frequency of the SQUID divided by $2e$, won't necessary need any quantum behaviour of the Josephson junctions. The peaks could arise due to Shapiro step like effect present in the asymmetric many Josephson junction system. The second part of the thesis concentrated on describing the system quantum mechanically and introducing the theory of an inelastic Cooper pair tunneling written explicitely for the many Josephson junction situation. We derived the current-voltage characteristics in the low temperature case for a single and also for a double SQUID environment. We also showed the connection between the gate voltage and the Bloch bands.

We concluded the thesis by analyzing two recent experiments for the voltage biased many Josephson junction system and the theoretical fits hinted that the quantum mechanical behaviour is the answer for those situations: the peaks in the experimental $I - V$ curve are probably a result from the macroscopic quantum states in the islands. However, there were problems in explaining all the peaks and their heights using the theory introduced in chapter 6. Also the gate voltage had no effect on the experimental $I - V$ curve when the Bloch bands were studied, which is in conflict with the theory. Therefore a deeper analysis of the dissipative prosesses, the effect of the temperature and the role of the quasicharge in these SSETs needs to be made if one wants to identify the Bloch bands from the experimental data (or the experimental situation has to be made more closer to the ideal one).

Bibliography

[1] A. O. Caldeira, A. J. Legget *Phys. Rev. Lett.* **46**, 211 (1981).

[2] A. J. Legget, A.Garg, *Phys. Rev. Lett.* **54**, 857 (1985).

[3] D. Vion, A. Aassime, A. Cottet, P. Joyez, H. Pothier, C. Urbina, D. Esteve, M. H. Devoret *Science* **296**, 886 (2002).

[4] M. Tinkham, *Introduction to Superconductivity*, 2nd ed. (New york: McGraw-Hill, 1996). Chapter 6.

[5] R. P. Feynman, R. B. Leighton, M. Sands, *The Feynman Lectures on Physics*, Vol. 3 (Reading, Massachusettes: Addison-Wesley, 1965). Chapter 21.

[6] B. D. Josephson, *Phys. Lett.* **1**, 251 (1962).

[7] P. W. Anderson, J. M. Rowell, *Phys. Rev. Lett.* **10**, 230 (1963).

[8] J. Bardeen, L. N. Cooper, J. R. Schrieffer, *Phys. Rev.* **108**, 1175 (1957).

[9] A more detailed treatment is given by B. D. Josephson, "weakly coupled superconductors" in *Superconductivity*, Vol. 1, R. D.Parks ed. (New york: Marcel Dekker, 1969).

[10] V. Ambegaokar, A. Baratoff, *Phys. Rev. Lett.* **10**, 486 (1963).

[11] S. Shapiro, *Phys. Rev. Lett.* **11**, 80 (1964).

[12] M. D. Fiske, *Rev. Mod. Phys.* **36**, 221 (1964).

[13] Jian-Xin Zhu, Z. Nussinov, A. V. Balatsky, arXiv:cond-mat/0306107 (2003).

[14] R. Lindell, J. Penttilä, M. Sillanpää, P. Hakonen, arXiv:cond-mat/0303536 (2003).

[15] see for example: L. D. Landau, E. M. Lifshift, *Course of Theoretical Physics*, Vol. 1, third ed. (Oxford: Butterworth-Heinemann 2001).

[16] K. K. Likharev, A. B. Zorin, *J. Low Temp. Phys.* **59**, 347 (1985).

[17] P. W. Anderson, in *Lectures on the Many-Body Problem*, Vol. 2, E. R. Caianiello ed. (Academic press, New York, 1964). P. 113.

[18] S. Washburn, R. A. Webb, R. F. Voss, S. M. Faris, *Phys. Rev. Lett.* **54**, 2712 (1985).

[19] M. H. Devoret, J. M Martinis, J. Clarke, *Phys. Rev. Lett.* **55**, 1908 (1985).

[20] J. M. Martinis, M. H. Devoret, J. Clarke, *Phys. Rev. Lett.* **55**, 1543 (1985).

[21] P. Silvestrini, V. G. Palmieri, B. Ruggiero, M. Russo, *Phys. Rev. Lett.* **79**, 3046 (1997).

[22] R. Rouse, S. Han, J. E. Lukens, *Phys. Rev. Lett.* **75**, 1614 (1995).

[23] see for example: M. P. Marder, *Condensed Matter Physics* (New York: John Wiley and Sons, 2000). P. 416.

[24] L. S. Kuzmin, D. B. Haviland, *Phys. Rev. Lett.* **67**, 2890 (1991).

[25] J. Delahaye, J. Hassel, R. Lindell, M. Sillanpää, M. Paalanen, H. Seppä, P. Hakonen, *Science* **299**, 1045 (2003).

[26] M. Iansiti, M. Tinkham, A.T. Johnson, W.F. Smith, C.J.Lobb, *Phys. Rev. B* **39**, 6465 (1989).

[27] A. Shinirman, G. Schön, Z. Herman, *Phys. Rev. Lett* **79**, 2371 (1997).

[28] *Single Charge Tunneling*, NATO ASI series Vol. B 294, edited by H. Grabert and M. H. Devoret, (Plenum Press, New York, 1992). Chapter 4.

[29] A. Wallraff, T. Duty, A. Lukashenko, A. V. Ustinov *Phys. Rev. Lett.* **90**, 037003 (2003).

[30] M. Tinkham, *Introduction to Superconductivity*, 2nd ed. (New york: McGraw-Hill, 1996). Chapter 7.

[31] E. Bibow, P. Lafarge, L. P. Levy, *Phys. Rev. Lett.* **88**, 017003 (2002).

[32] J. M. Martinis, M. H. Devoret, J. Clarke, *Phys. Rev. B* **35**, 4682 (1987).

[33] G. L. Ingold and Y. V. Nazarov, *Single Charge Tunneling*, ed. H. Grabert and M. H. Devoret (Plenum, New York, 1992). Chapter 2.

[34] D. B. Haviland, L. S. Kuzmin, P. Delsing, T. Claeson, *Europhys. Lett.* **16**, 103 (1991).

[35] L. J. Geerlings, J. Romijn, V. F. Anderegg, J. E. Mooij, *Phys. Rev. Lett.* **65** 377 (1990).

[36] G. L. Ingold, H. Grabert, *Phys. Rev. B* **50**, 395 (1994).

[37] T. Holst, D. Esteve, C. Urbina, M. H. Devoret, *Phys. Rev. Lett.* **25**, 3455 (1994). T. Holst, D. Esteve, C. Urbina, M. H. Devoret, *Physica B* **203**, 397 (1994).

[38] G. L. Ingold, H. Grabert, *Europhys. Lett.* **14**, 395 (1991).

[39] G. Schön, A. D. Zaikin, *Physics Reports* **198**, 237-412 (1990).

[40] R. Lindell, *Spectroscopy in Ultrasmall Josephson Junction using Inelastic Cooper Pair tunneling*, Master's Thesis, Helsinki University of Technology, (2001).

[41] R. Lindell, J. Penttilä, M. Paalanen, P. Hakonen, *Physica E* **18**, 13 (2003).

[42] D. V. Averin, K. K. Likharev, in *Mesoscopic Phenomena in Solids*, ed. B. L. Altshuler, P. A. Lee, R. A. Webb, (Elsevier 1991). P. 173

[43] M. Watanabe, D. B. Haviland *Phys. Rev. B* **67**, 094505 (2003).

[44] M. Watanabe, D. B. Haviland *Phys. Rev. Lett.* **86**, 5120 (2001).

[45] J. Siewert, G. Schön, *Phys. Rev. B* **54**, 7421 (1996).

[46] Y. Harada, A. A. Odintsov *Phys. Rev. B* **54**, 6608 (1996).

[47] K. A. Matveev, M. Gisselfält, L. I. Glazman, M. Jonson, R. I. Shekhter, *Phys. Rev. Lett.* **70**, 2940 (1993).

[48] A. M. v. d. Brink, G. Schön, L. J. Geerligs, *Phys. Rev. Lett.* **67**, 3030 (1991).

[49] see for example: S. Zhang, J. Jin, *Computation of Special Functions*, (John-Wiley and Sons Inc., New York, 1996).